*Research Article*

# Comparison between Heat-Clearing Medicine and Antirheumatic Medicine in Treatment of Gastric Cancer Based on Network Pharmacology, Molecular Docking, and Tumor Immune Infiltration Analysis

**Jiamin Xu** [iD],[1] **Fuqin Kang,**[2] **Wei Wang,**[3] **Shujun Liu,**[1]
**Jianhui Xie** [iD],[4,5,6] **and Xiaobo Yang** [iD][4,5,6]

[1]*State Key Laboratory of Dampness Syndrome of Chinese Medicine, The Second Clinical College of Guangzhou University of Chinese Medicine, Guangzhou, China*
[2]*The Second Clinical College of Guangzhou University of Chinese Medicine, Guangzhou, China*
[3]*Gastrointestinal Surgery, Guangdong Provincial Hospital of Chinese Medicine, Guangzhou, China*
[4]*State Key Laboratory of Dampness Syndrome of Chinese Medicine, The Second Affiliated Hospital of Guangzhou University of Chinese Medicine, Guangzhou, China*
[5]*Guangdong Provincial Key Laboratory of Clinical Research on Traditional Chinese Medicine Syndrome, Guangzhou, China*
[6]*The Second Affiliated Hospital, Guangzhou University of Chinese Medicine, Guangzhou, China*

Correspondence should be addressed to Xiaobo Yang; yangxiaobo39358517@hotmail.com

*Background.* Clinical research found that TCM is therapeutic in treating gastric cancer. Clearing heat is the most common method, while some antirheumatic medicines are widely used in treatment as well. To explore the pharmacological mechanism, we researched the comparison between heat-clearing medicine and antirheumatic medicine in treating gastric cancer. *Methods.* First, related ingredients and targets were searched, respectively, and are shown in an active ingredient-target network. Combining the relevant targets of gastric cancer, we constructed a PPI network and MCODE network. Then, GO and KEGG enrichment analyses were conducted. Molecular docking experiments were performed to verify the affinity of targets and ligands. Finally, we analyzed the tumor immune infiltration on gene expression, somatic CNA, and clinical outcome. *Results.* A total of 31 ingredients and 90 targets of heat-clearing medicine, 31 ingredients and 186 targets of antirheumatic medicine, and 12,155 targets of gastric cancer were collected. Antirheumatic medicine ranked the top in all the enrichment analyses. In the KEGG pathway, both types of medicines were related to pathways in cancer. In the KEGG map, AR, MMP2, ERBB2, and TP53 were the most crucial targets. Key targets and ligands were docked with low binding energy. Analysis of tumor immune infiltration showed that the expressions of AR and ERBB2 were correlated with the abundance of immune infiltration and made a difference in clinical outcomes. *Conclusions.* Quercetin is an important ingredient in both heat-clearing medicine and antirheumatic medicine. AR signaling pathway exists in both types of medicines. The mechanism of the antitumor effect in antirheumatic medicine was similar to trastuzumab, a targeted drug aimed at ERBB2. Both types of medicines were significant in tumor immune infiltration. The immunology of gastric tumor deserves further research.

## 1. Introduction

According to the data of the International Agency for Research on Cancer (IARC) [1] in 2020, there were about 1.089 million new gastric cancer cases all over the world, ranking fifth among malignant tumors. In 2020, 769 thousand people died from gastric cancer and 48.6% of death took place in China. High morbidity and mortality of gastric cancer are huge burdens to the Chinese medical system. For early-stage gastric cancer, endoscopic resection, surgery, and

chemoradiotherapy are clinically recommended. However, surgery and chemoradiotherapy are not suitable for all patients with gastric cancer [2]. Tumor invasion, lymph node metastases, distant metastasis, and peritoneal implantation are not suitable for surgery. Chemoradiotherapy is not recommended to patients in poor general condition, hypoproteinemia, anemia, malnutrition, and underlying diseases [3–7]. Systemic antitumor therapy is the only option left for situations mentioned above, which generally include chemotherapeutic and molecular targeted drugs. Several trials showed that those therapeutics could not improve overall survival and had significant toxicities [8–13]. The common toxicities include neutropenia, anorexia, anemia, nausea, and vomiting. It is hard to balance the benefits and risks. What's more, due to the lack of adequate medical knowledge and regular physical examination, most gastric cancers are at an advanced stage once detected.

Recent clinical research found that traditional Chinese medicine (TCM) is therapeutic in the treatment of gastric cancer. TCM shows advantages of lowering recurrence rate, preventing adverse reactions of chemoradiotherapy, prolonging survival, and clinically strengthening immunity. Ma and Liu [14] found that formula for heat-clearing medicine and benefiting qi had a better clinical efficacy rate, Karnofsky score, quality of survival, and fewer adverse reactions, compared with DCF chemotherapy. Both Th17 and Treg cells are subsets of CD4+ T cell. Th17 secretes proinflammatory factors (IL-17), while Treg secretes anti-inflammatory factors (IL-10 and TGF-$\beta$). Th17, Treg cells, and the rate of Th17/Treg significantly decreased after TCM therapy, which means the mechanism of treating cancer with TCM might be related to immunity and inflammation [15, 16]. One clinical study for advanced gastric cancer found that formula for heat-clearing and dissipating phlegm had better efficacy and health status than general chemotherapy [17]. After 4-week therapy, IL-6, IL-8, TNF-$\alpha$, and CRP remarkably reduced. It revealed that TCM therapy might be associated with anti-inflammatory and metabolic processes.

Clearing heat is a common TCM method for treating cancer. Based on theories of TCM, heat-clearing medicine is a typical type of medicine with a cool attribute and effects of clearing heat and removing toxicity. Recent pharmacological studies have shown that heat-clearing medicines could remove pathogenic microorganisms, endotoxicity, inflammation, and enhance immunity [18–20]. Besides, some medicines are broadly clinically used in both cancer and rheumatic diseases. Some latest studies found that immunity and inflammation are important features of cancer [21, 22]. Cytokines such as interleukin (IL), chemokines, and lymphocytes play a key role in tumor biology and pathology [23–25]. Tumor microenvironment (TME) consists of tumor cells, fibroblasts, immune cells, glial cells, and other acellular components [26, 27]. For example, the expression of IL-6 expression is closely related to tumor stage, metastasis, and prognosis. Higher plasma IL-6 level often clinically indicates advanced and metastasis tumor [28]. In addition, studies of IL-1$\beta$, IL-11, IL-17, IL-18, and TNF also indicate that proinflammatory cytokines are key regulators for TME in inhibiting tumor cell proliferation, reducing inflammation, and preventing tumor metastasis [29, 30].

Some researchers explored the ingredients and antitumor activities of *Tripterygii Radix*, *Actinidia chinensis Planch*, *Polygoni Cuspidati Rhizoma Et Radix*, and so on. In an in vitro experiment, Arora et al. found that triptolide could decrease the viability of gastric cancer cells and increase apoptosis [31]. Lei et al. isolated cisresveratrol and transresveratrol from *Polygoni Cuspidati Rhizoma Et Radix* and found tumor growth inhibition of resveratrol [32]. The extract of *Actinidia chinensis Planch* was proved to inhibit the proliferation and metastasis of gastric cancer cells [33–35]. However, no study focused on the association between the category of antirheumatic medicine and cancer. To explore this issue, we hypothesized that the antitumor mechanism of general heat-clearing medicines was different from antirheumatic herbal medicines.

Network pharmacology is a multidisciplinary method that integrates medicine, biology, and bioinformatics. This method could provide an insight into the complex mechanisms of TCM on diseases, which conforms to the multicomponent, multitarget, and multipathway of TCM. Computer-aided learning could simulate computer operation to predict the interactions between molecules and targets at a molecular level, which is widely used in pharmaceutical research. Some researchers explored the association between TCM and diabetes using network analysis and molecular docking [36]. Oh et al. investigated the bioactivities of *Zanthoxylum piperitum* fruits in treating rheumatoid arthritis based on network pharmacology [37]. Previous studies showed that computer-aided learning is an appropriate method for pharmaceutical research.

Therefore, we did research based on network pharmacology to find the key ingredients and targets. Then molecular docking experiment was performed to validate the interaction activity of key proteins and ligands. Finally, to verify the association of immunity and gastric cancer, analysis of tumor immune infiltration was operated based on The Cancer Genome Atlas (TCGA). The flow diagram is shown in Figure 1.

## 2. Method

### 2.1. Searching and Screening Related Ingredients and Targets.
According to the classification of Chinese materia medica, representative medicine of gastric cancer was selected in this research. *Oldenlandia diffusa* (Chinese Pinyin name: Baihuasheshecao), *Scutellaria barbata* (Chinese Pinyin name: Ban zhi lian), and *Taraxacum mongolicum* (Chinese Pinyin name: Pugongying) represented the commonly used heat-clearing medicine. The typical antirheumatic herbal medicines were *Rabdosia rubescens* (Chinese Pinyin name: Dong ling cao), *Duchesnea indica* (Chinese Pinyin name: Shemei), *Smilax glabra* (Chinese Pinyin name: Tufuling), *Akebia quinata* (Chinese Pinyin name: Yuzhizi), and *Actinidia chinensis Planch* (Chinese Pinyin name: Tengligen). The ingredients of herbal medicines mentioned above were searched through the traditional Chinese medicine systems pharmacology database and analysis platform (TCMSP database https://old.tcmsp-e.com/tcmsp.php) and anticancer herbs database of systems pharmacology (CancerHSP
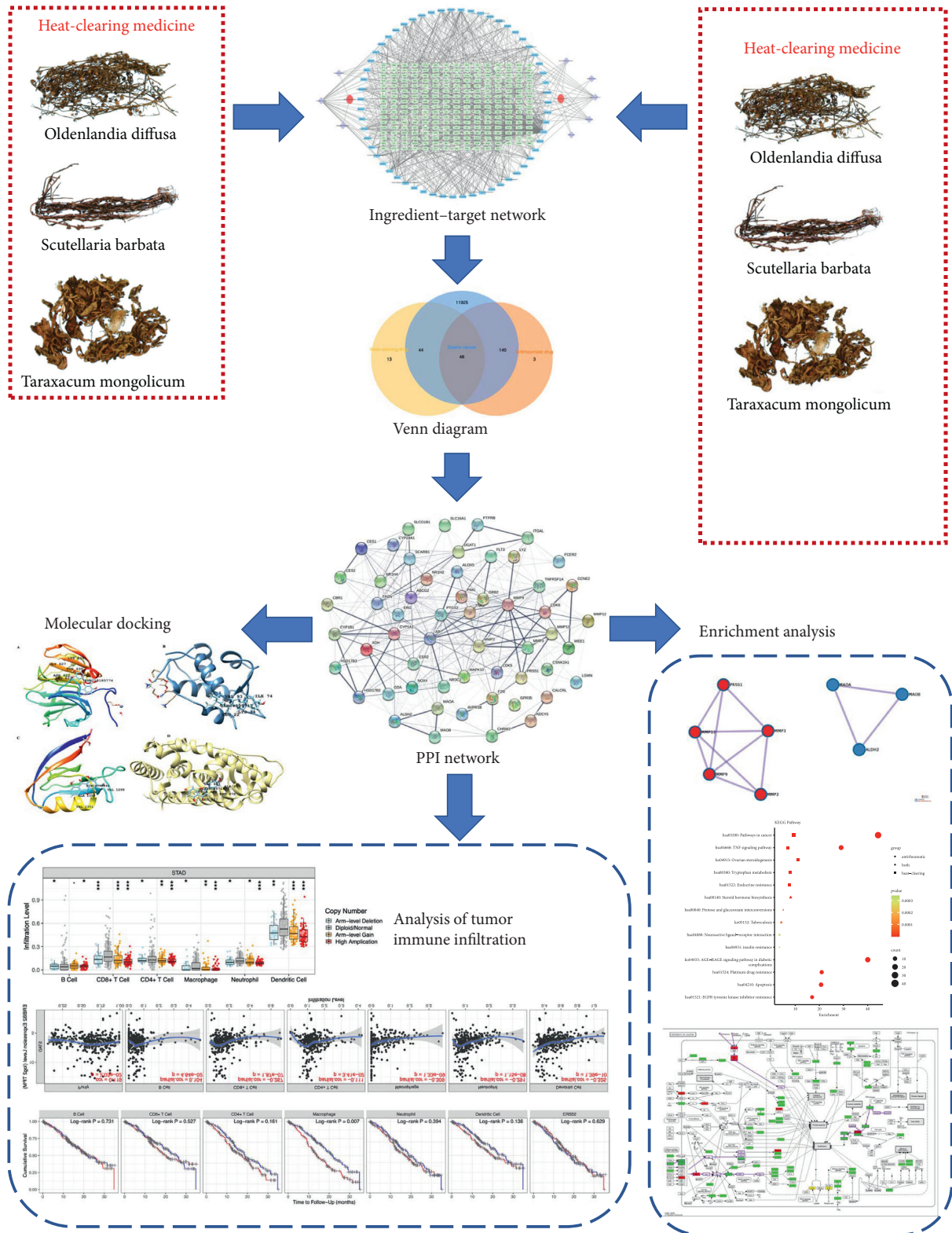
FIGURE 1: Schematic flow diagram: searching medicines, constructing ingredient-target network, Venn diagram, PPI network, enrichment analysis, molecular docking, and analysis of tumor immune infiltration.

database https://old.tcmsp-e.com/CancerHSP.php) [38]. Two ADME values including oral availability (OB) ≥30% and drug likeness (DL) ≥0.18 were screened for eligible

ingredients. We also searched related ingredients from the PubMed database according to relative articles. According to ingredients collected before, we obtained targets from the

TCMSP database, CancerHSP database, and relative articles in the same way mentioned above. To standardize the information of targets, we unified all the included targets based on the UniProt protein database (https://www.uniprot.org) [39].

*2.2. Constructing an Active Ingredient-Target Network.* The active ingredient-target network of heat-clearing medicine and antirheumatic medicine was constructed and analyzed through Cytoscape 3.8.1 [40]. Nodes denoted ingredients or targets. Edges represented that some ingredients could activate or inhibit the connected targets, according to previous studies. The Network Analyzer tool in Cytoscape calculated the characteristic parameters in a network, including degree, betweenness, and closeness.

*2.3. Searching and Screening Related Targets of Gastric Cancer.* To ensure that relevant targets of gastric cancer were comprehensive in this study, we searched in four gene databases, including GeneCards database [41] (https://www.genecards.org), OMIM database [42] (https://www.omim.org), TTD database [43] (https://bidd.nus.edu.sg/group/cjttd), and DrugBank database [44] (https://www.drugbank.ca). Relevant targets were downloaded from databases and integrated as a dataset about gastric cancer.

*2.4. Constructing PPI Network.* To clarify the relationship between heat-clearing medicine, antirheumatic medicine, and gastric cancer, a protein-protein interaction (PPI) network was constructed in the STRING 11.0 database [45, 46] (https://string-db.org). Biological species were limited to Homo sapiens, and the minimum interaction threshold was set as the highest confidence (>0.9). After constructing the PPI network, the potential protein functional modules and biological processes were analyzed by applying the molecular complex detection (MCODE) algorithm [47]. Using the MCODE plugin and its default parameters in Cytoscape software, the MCODE algorithm could identify neighborhoods of densely connected proteins by clustering and classifying proteins.

*2.5. Enrichment Analysis.* Gene Ontology (GO) [48] enrichment and Kyoto Encyclopedia of Genes and Genomes (KEGG) [49] enrichment were analyzed in Metascape [50] (https://metascape.org). Molecular function, biological process, cellular component, and KEGG pathway were analyzed and selected with a $p$-value <0.01, a minimum count of 3, and an enrichment factor >1.5. The results were visualized in R software.

*2.6. Molecular Docking.* The three-dimensional structure of ligands was built in ChemOffice [51] software and saved in MOL2 format of minimized energy. The 3D structures of targets were downloaded from Protein Data Bank (PDB) [52] (https://www.rcsb.org/). PyMOL software [53] was used to remove water and add hydrogen to the target. We performed blind docking of ligands and targets in AutoDock Vina software [54]. The three coordinates of the grid box were adjusted to enclose the whole protein. AutoDock Vina calculated all the possible binding residues and presented the parameter containing residues, binding energy, cluster, and so on.

*2.7. Analysis of Tumor Immune Infiltration.* In the TIMER database [55] (https://cistrome.shinyapps.io/timer/), the deconvolution algorithm could estimate the correlation between gene expression and abundances of six immune infiltrates (B cells, CD4+ T cells, CD8+ T cells, neutrophils, macrophages, and dendritic cells). GISTIC 2.0 [56, 57] could identify regions of the genome that are significantly amplified or deleted across a set of samples. In this study, the association between immune infiltrates and somatic copy number alterations (SCNAs) of a gene across TCGA cancer types was evaluated in GISTIC 2.0. Based on The Cancer Genome Atlas (TCGA) database [58] (https://portal.gdc.cancer.gov), prediction of clinical outcome and abundance of immune infiltrates were calculated in a multivariable Cox proportional hazard model.

# 3. Result

*3.1. Active Ingredients and Relevant Targets of Medicines.* Ingredients were selected based on oral availability and drug likeness for good absorption, distribution, metabolism, and excretion in vivo. A total of 31 active ingredients of heat-clearing medicine and 31 active ingredients of antirheumatic medicine were collected from the TCMSP database, CancerHSP database, and related articles (Table 1). There were 90 relevant targets of heat-clearing medicine and 186 relevant targets of antirheumatic medicine (Supplementary Table 1).

*3.2. Ingredient-Target Network.* The ingredient-target network of heat-clearing medicine and antirheumatic medicine was constructed in Cytoscape 3.8.1. As shown in Figure 2, two red ellipses represented two types of medicines, and eight diamonds denoted medicines. Blue rectangles were active ingredients and green ones were relevant targets. The gray lines showed us the relationship between medicines, ingredients, and targets. The network topological parameters including degree, betweenness, and closeness are shown in Table 2.

*3.3. Relevant Targets of Gastric Cancer.* There were 12,155 targets in the GeneCards database, 427 targets in the OMIM database, 42 targets in the TTD database, and 32 targets in the DrugBank database. Gastric cancer-relevant targets were collected, respectively, which were deduplicated and integrated as a dataset containing 12,155 targets (Supplementary Table 2).

*3.4. Protein-Protein Interaction Network.* With all the relevant targets of medicines and gastric cancer, we constructed a Venn diagram to display the relationship (shown in

Table 1: The relevant ingredients of medicines.

| Type | Medicine | Ingredient | Ingredient | Ingredient |
|---|---|---|---|---|
| Heat-clearing medicine | Oldenlandia diffusa | Oleanolic acid | Oleanolic acid | VDR, HSD11B2, CYP27B1, AKR1B10, POLB, PLA2G1B, PTPN1, RXRA, CYP17A1, SRD5A1, DUOX2, UGT2B7 |
| | | Ursolic acid | Ursolic acid | VDR, HSD11B2, AKR1B1, CYP19A1, POLB, PTPN1, PTPN6, PTPRA, PTPRE, RXRA, CYP17A1, SRD5A1, PTPN2, DUOX2, UGT2B7 |
| | | 10(S)-hydroxypheophytin a | 10(S)-hydroxypheophytin a | CYP24A1, FNTA, GRB2, WEE1, CALCRL, ELOVL6, FCER2, LGMN, RIOK2, TNK2, BIRC7, CCL5, DUOX2, HPSE, HSD11B2, KISS1R, LNPEP, NR3C1, PGC, PPP3CA, SFRP1, SLC10A2, SPHK1, VDR |
| | | 6-O-(E)-p-coumaroyl scandoside methyl ester | 6-O-(E)-p-coumaroyl scandoside methyl ester | AVPR1B, F2R, SLCO1B1, ITGAL, GLB1, LNPEP, OGA, YARS1 |
| | Scutellaria barbata | Apigenin | Apigenin | ABCG2, ADCY5, ALDH2, ALOX5, CBR1, CDK5, CES2, CYP1A1, CYP1B1, FLT3, GDA, HSD17B3, MAOA, MAOB, MAPK10, MECR, NOX4, PIM1, PLAA, PTGS2, TNFRSF1A, TNKS2, XDH, AR, CDK6, CSNK2A1, ESR2, HSD17B2, LYZ, CYP2A6, CYP19A1 |
| | | Barbatellarine B | Barbatellarine B | AVPR1B, F2R, PTPRB, SLC16A1, CYP27B1, FKBP5, HSD11B2, KISS1R, NR3C1, PGC, SLC10A2, SRD5A1, VDR |
| | | Barbatin A | Barbatin A | AVPR1B, F2R, FNTA, NR1H4, SLCO1B1, BIRC7, CYP27B1, FKBP5, HSD11B2, KISS1R, NR3C1, SFRP1, SLC10A2, SRD5A1 |
| | | Barbatin B | Barbatin B | AVPR1B, FNTA, PTPRB, SLC16A1, BIRC7, CYP27B1, FKBP5, HSD11B2, KISS1R, NR3C1, PGC, SFRP1, SLC10A2, SRD5A1, VDR |
| | | Barbatin C | Barbatin C | CYP17A1, CYP27B1, GLB1, HSD11B2, NR3C1, SRD5A1, UGT2B7, VDR |
| | | Barbatin D | Barbatin D | AVPR1B, CYP24A1, F2R, FNTA, NR1H2, PTPRB, SLC16A1, SLCO1B1, BIRC7, CYP27B1, FKBP5, HSD11B2, KISS1R, NR3C1, RASGRP3 |
| | | Barbatin E | Barbatin E | AVPR1B, FNTA, NR1H4, PTPRB, SLCO1B1, CES1, BIRC7, CYP27B1, DUOX2, FKBP5, HSD11B2, NR3C1, PGC, RASGRP3, SFRP1, SLC10A2, VDR |
| | | Pheophorbide a | Pheophorbide a | AVPR1B, GRB2, NR1H2, PTPRB, SLC16A1, WEE1, NR3C2, PDE1B, SCARB1, BIRC7, FKBP5, HSD11B2, KISS1R, LNPEP, MLNR, NR3C1 |
| | | Scutebarbatine B | Scutebarbatine B | AVPR1B, CYP24A1, F2R, FNTA, NR1H2, NR1H4, PTPRB, SLC16A1, SLCO1B1, BIRC7, CYP27B1, FKBP5, HSD11B2, KISS1R, NR3C1, RASGRP3 |
| | | Scutebarbatine C | Scutebarbatine C | AVPR1B, CHRM2, FNTA, NR1H4, PTPRB, SLC16A1, SLCO1B1, CYP27B1, FKBP5, HSD11B2, KISS1R, NR3C1, SFRP1, SLC10A2, SRD5A1, VDR |
| | | Scutebarbatine D | Scutebarbatine D | AVPR1B, CHRM2, F2R, FNTA, NR1H4, PTPRB, SLC16A1, SLCO1B1, CYP27B1, FKBP5, HSD11B2, KISS1R, MLNR, NR3C1, SLC10A2, SRD5A1 |
| | | Luteolin | Luteolin | ABCG2, ADCY5, ALDH2, ALOX5, CBR1, CDK5, CES2, CYP1A1, CYP1B1, FLT3, GDA, HSD17B3, MAOA, MAOB, MAPK10, MECR, NOX4, PIM1, PLAA, TNFRSF1A, TNKS2, XDH, ABCB1, CCNE2, FASN, GPR35, KDM4E, LAP3, MMP12, MMP13, MMP2, MMP3, MMP9, PRSS1 |
| | | Scutebarbatine G | Scutebarbatine G | F2R, FNTA, SLC16A1, BIRC7, CYP27B1, HSD11B2, SLC10A2, SRD5A1, UGT2B7, VDR |
| | | Scutebarbatine H | Scutebarbatine H | FNTA, PTPRB, BIRC7, CYP27B1, HSD11B2, NR3C1, SLC10A2, SRD5A1, UGT2B7, VDR |
| | | Scutebata A | Scutebata A | AVPR1B, F2R, FNTA, PTPRB, CCL5, CYP27B1, FKBP5, HSD11B2, KISS1R, NR3C1, PGC, SFRP1, SLC10A2, SRD5A1 |
| | | Scutehenanine A | Scutehenanine A | FNTA, SLC16A1, BIRC7, CYP27B1, HSD11B2, NR3C1, RASGRP3, SRD5A1, VDR |
| | | Scutehenanine B | Scutehenanine B | AVPR1B, ERG, F2R, FNTA, SLC16A1, SLCO1B1, BIRC7, CYP27B1, FKBP5, HSD11B2, KISS1R, NR3C1, RASGRP3, SFRP1, SLC10A2, SRD5A1, UGT2B7, VDR |
| | | Scutehenanine C | Scutehenanine C | AVPR1B, ERG, F2R, FNTA, SLCO1B1, CCL5, CYP27B1, FKBP5, HSD11B2, KISS1R, NR3C1, PGC, RASGRP3, SFRP1, SLC10A2, SRD5A1, UGT2B7, VDR |
| | | Scutehenanine D | Scutehenanine D | AVPR1B, F2R, FNTA, NR1H4, PTPRB, SLCO1B1, BIRC7, CYP27B1, FKBP5, HSD11B2, KISS1R, NR3C1, RASGRP3, SLC10A2, SRD5A1, VDR |
| | | Scutellarin | Scutellarin | GRB2, GLB1, HTR2A, OGA, SLC5A2, YARS1 |
| | | Wogonin | Wogonin | ADCY5, ALDH2, CBR1, CES2, GDA, PTGS2 |
| | | 6,7-di-O-nicotinoylscutebarbatine G | 6,7-di-O-nicotinoylscutebarbatine G | AVPR1B, F2R, FNTA, SLC16A1, BIRC7, CYP27B1, FKBP5, HSD11B2, KISS1R, NR3C1, PGC, SFRP1, SLC10A2, SRD5A1, VDR |
| | | 6-O-(2-carbonyl-3-methylbutanoyl) scutehenanine A | 6-O-(2-carbonyl-3-methylbutanoyl) scutehenanine A | AVPR1B, F2R, FNTA, NR1H2, PTPRB, SLC16A1, SLCO1B1, BIRC7, CYP27B1, FKBP5, HSD11B2, KISS1R, NR3C1, RASGRP3, SFRP1, SLC10A2, VDR |
| | | 6-O-acetylscutehenanine A | 6-O-acetylscutehenanine A | AVPR1B, FNTA, BIRC7, CYP27B1, HSD11B2, NR3C1, RASGRP3, SLC10A2, SRD5A1, VDR |
| | | 6-O-nicotinoyl-7-O-acetylscutebarbatine G | 6-O-nicotinoyl-7-O-acetylscutebarbatine G | AVPR1B, F2R, CYP27B1, FKBP5, HSD11B2, KISS1R, NR3C1, PGC, RASGRP3, SFRP1, SLC10A2, SRD5A1 |
| | | 7-O-nicotinoylscutebarbatine H | 7-O-nicotinoylscutebarbatine H | AVPR1B, F2R, FNTA, PTPRB, SLC16A1, SLCO1B1, CYP27B1, HSD11B2, KISS1R, NR3C1, RASGRP3, SLC10A2, SRD5A1, VDR |
| | Taraxacum mongolicum | Chlorogenic acid | Chlorogenic acid | GLB1, OGA, YARS1 |

Table 1: Continued.

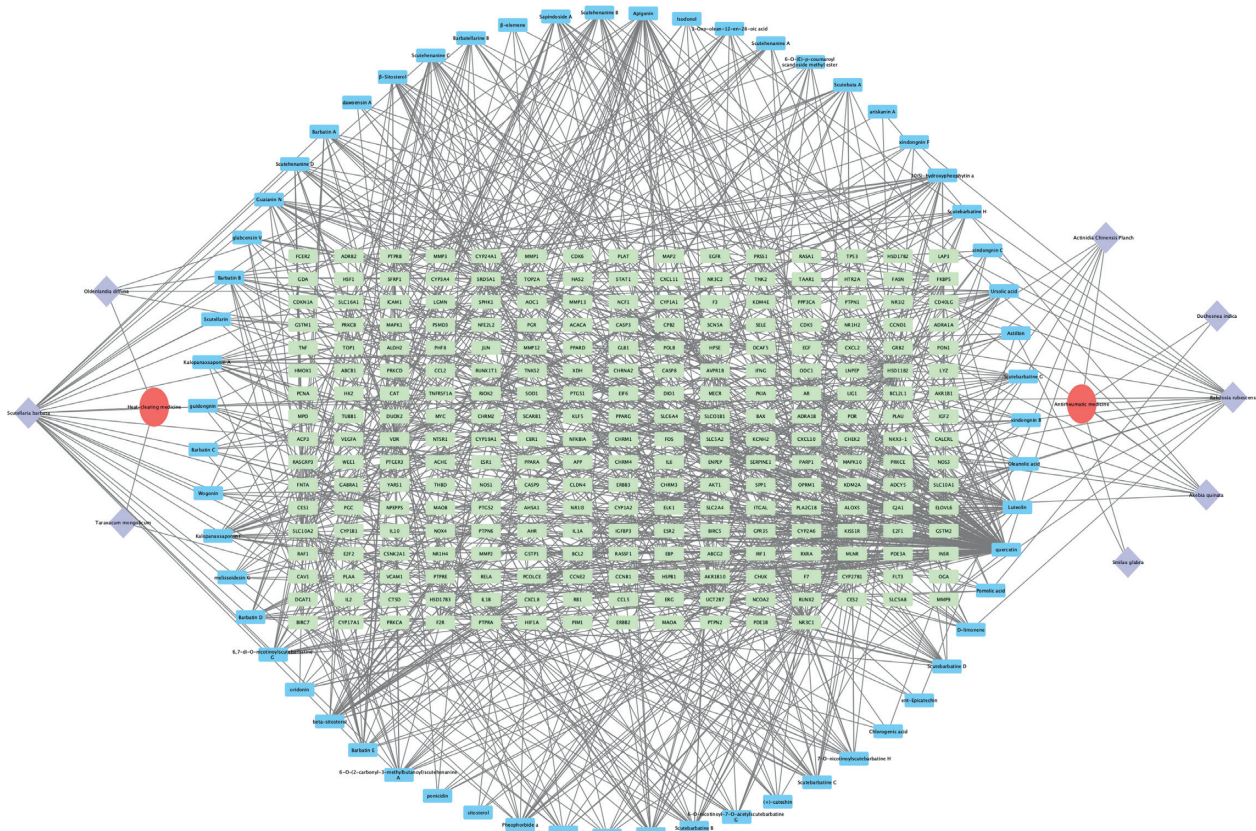| Type | Medicine | Ingredient | Ingredient |
|---|---|---|---|
| | | D-limonene | AOC1, EBP, ENPEP, CPB2, KDM2A, LIG1, NOS1, PHF8, TAAR1, CYP2A6 |
| | | Xindongnin B | CYP27B1, GLB1, HSD11B2, RASGRP3, SLC10A2, SRD5A1, UGT2B7, VDR |
| | | Xindongnin C | SLC5A8, CYP27B1, HSD11B2, SRD5A1, UGT2B7, VDR |
| | | Xindongnin F | GLB1, HSD11B2, SRD5A1, UGT2B7, VDR |
| | | Oleanolic acid | VDR, HSD11B2, CYP27B1, AKR1B10, POLB, PLA2G1B, PTPN1, RXRA, CYP17A1, SRD5A1, DUOX2, UGT2B7 |
| | | Ursolic acid | VDR, HSD11B2, AKR1B1, CYP19A1, POLB, PTPN1, PTPN6, PTPRA, PTPRE, RXRA, CYP17A1, SRD5A1, PTPN2, DUOX2, UGT2B7 |
| | Rabdosia rubescens | Isodonol | CYP27B1, GLB1, HSD11B2, SLC10A2, SRD5A1, UGT2B7 |
| | | β-elemene | AOC1, EBP, ENPEP, VDR |
| | | Dawoensin A | CYP27B1, HSD11B2, SRD5A1, UGT2B7, VDR |
| | | Glabcensin V | CYP27B1, HSD11B2, RASGRP3, SLC10A2, SRD5A1, UGT2B7, VDR |
| | | Guidongnin | CYP27B1, HSD11B2, NR3C1, RASGRP3, SLC10A2, SRD5A1, UGT2B7, VDR |
| | | Melissoidesin G | CYP27B1, HSD11B2, RASGRP3, SLC10A2, SRD5A1, UGT2B7, VDR |
| | | Oridonin | CYP27B1, GLB1, HSD11B2, SLC10A2, SRD5A1, UGT2B7 |
| | | Ponicidin | CYP27B1, HSD11B2, SFRP1, SRD5A1, UGT2B7 |
| | | Xindongnin A | BIRC7, CYP27B1, HSD11B2, NR3C1, SLC10A2, SRD5A1, UGT2B7, VDR |
| | | Pomolic acid | RXRA, CYP17A1, DUOX2, HSD11B2, SFRP1, UGT2B7, PTPN1 |
| | | Astilbin | GLB1, HTR2A, LNPEP, OGA, SLC5A2, YARS1 |
| | Duchesnea indica | Ariskanin A | SLC5A8, TUBB1 |
| | Smilax glabra | Oleanolic acid | VDR, HSD11B2, CYP27B1, AKR1B10, POLB, PLA2G1B, PTPN1, RXRA, CYP17A1, SRD5A1, DUOX2, UGT2B7 |
| | | 3-Oxo-olean-12-en-28-oic acid | RXRA, CYP17A1, CYP27B1, DUOX2, HSD11B2, SFRP1, SLC10A2, SRD5A1, UGT2B7, VDR |
| | | Sapindoside A | DGAT1, BIRC7, DUOX2, FKBP5, GLB1, HPSE, HSD11B2, KISS1R, LNPEP, MLNR, NR3C1, PGC, PPP3CA, SFRP1, SPHK1, SRD5A1, UGT2B7, VDR |
| Antirheumatic medicine | | β-Sitosterol | DGAT1, EBP, APP, KLF5, SLC10A1, CYP17A1, CYP27B1, DUOX2, HSD11B2, NR3C1, SPHK1, SRD5A1, UGT2B7, VDR, POLB |
| | Akebia quinata | Guaianin N | DUOX2, FKBP5, HPSE, HSD11B2, KISS1R, MLNR, NR3C1, PGC, PPP3CA, SFRP1, SLC10A2, SRD5A1, UGT2B7, VDR |
| | | Kalopanaxsaponin A | DGAT1, DUOX2, FKBP5, GLB1, HPSE, HSD11B2, KISS1R, LNPEP, MLNR, NR3C1, PGC, SFRP1, SPHK1, SRD5A1, UGT2B7, VDR |
| | | Kalopanaxsaponin I | NTSR1, CCL5, DUOX2, FKBP5, HPSE, HSD11B2, KISS1R, LNPEP, MLNR, NR3C1, OGA, PGC, PPP3CA, SFRP1, SPHK1, SRD5A1, UGT2B7, VDR |
| | | Beta-sitosterol | ADRA1A, ADRA1B, BAX, BCL2, ADRB2, CASP3, CASP8, CASP9, PDE3A, GABRA1, MAP2, OPRM1, CHRM1, CHRM2, CHRM3, CHRM4, CHRNA2, NCOA2, KCNH2, PGR, PTGS1, PTGS2, PRKCA, PON1, SCN5A, SLC6A4, JUN |
| | | Sitosterol | PGR, NCOA2, NR3C2 |
| | | Aloe-emodin | PTGS1, PTGS2, NCOA2, PKIA, CDKN1A, EIF6, BAX, TNF, CASP3, TP53, FASN, PRKCA, PRKCE, PCNA, MYC, IL1B, PRKCD, CCNB1 |
| | | (+)-catechin | PTGS1, ESR1, PTGS2, NCOA2, RXRA, CAT, HAS2 |
| | | Ent-epicatechin | PTGS1, ESR1, PTGS2 |
| | Actinidia chinensis Planch | Quercetin | PTGS1, AR, PTGS2, NCOA2, PRSS1, KCNH2, SCN5A, ADRB2, MMP3, F7, RXRA, ACHE, GABRA1, MAOB, RELA, EGFR, AKT1, VEGFA, CCND1, BCL2, BCL2L1, FOS, CDKN1A, EIF6, BAX, CASP9, PLAU, MMP2, MMP9, MAPK1, IL10, EGF, RB1, TNF, JUN, IL6, AHSA1, CASP3, TP53, ELK1, NFKBIA, POR, ODC1, CASP8, TOP1, RAF1, SOD1, PRKCA, MMP1, HIF1A, STAT1, RUNX1T1, ERBB2, PPARG, ACACA, HMOX1, CYP3A4, CYP1A2, CAV1, MYC, F3, GJA1, CYP1A1, ICAM1, IL1B, CCL2, SELE, VCAM1, PTGER3, CXCL8, PRKCB, BIRC5, DUOX2, NOS3, HSPB1, IL2, NR1I2, CYP1B1, CCNB1, PLAT, THBD, SERPINE1, IFNG, IL1A, MPO, TOP2A, NCF1, HAS2, GSTP1, NFE2L2, PARP1, AHR, PSMD3, SLC2A4, CXCL11, CXCL2, DCAF5, NRI13, CHEK2, INSR, CLDN4, PPARA, PPARD, HSF1, CXCL10, CHUK, SPP1, RUNX2, RASSF1, E2F1, E2F2, ACP3, CTSD, IGFBP3, IGF2, CD40LG, IRF1, ERBB3, PON1, DIO1, PCOLCE, NPEPPS, HK2, NKX3-1, RASA1, GSTM1, GSTM2 |

FIGURE 2: Ingredient-target network of heat-clearing medicine and antirheumatic medicine. The red ellipses, purple diamonds, blue rectangles, and green rectangles represent two types of medicines, eight medicines, 62 ingredients, and 825 targets, respectively. The gray lines denote their relationship.

TABLE 2: Network topological parameters.

|  | Name | Degree | Betweenness | Closeness |
|---|---|---|---|---|
| Target | HSD11B2 | 43 | 5407.4346 | 0.3171 |
|  | SRD5A1 | 36 | 2855.4278 | 0.3033 |
|  | CYP27B1 | 34 | 1962.1760 | 0.2977 |
|  | VDR | 33 | 3799.5332 | 0.3092 |
|  | NR3C1 | 29 | 1692.5265 | 0.2999 |
|  | SLC10A2 | 27 | 1111.4990 | 0.2944 |
|  | UGT2B7 | 25 | 1637.7742 | 0.2901 |
|  | KISS1R | 21 | 823.8508 | 0.2875 |
|  | FKBP5 | 20 | 642.3051 | 0.2839 |
|  | AVPR1B | 19 | 512.6839 | 0.2805 |
| Ingredient | Quercetin | 128 | 62208.7944 | 0.4178 |
|  | Luteolin | 35 | 11794.5504 | 0.3194 |
|  | Apigenin | 32 | 12547.0981 | 0.3412 |
|  | Beta-sitosterol | 28 | 8122.2824 | 0.2980 |
|  | 10(S)-hydroxypheophytin a | 25 | 7106.1379 | 0.3239 |
|  | Kalopanaxsaponin I | 19 | 3471.1257 | 0.3219 |
|  | Aloe-emodin | 19 | 3255.0639 | 0.2862 |
|  | Sapindoside A | 19 | 2787.3090 | 0.3219 |
|  | Scutehenanine C | 19 | 935.7868 | 0.2740 |
|  | Scutehenanine B | 19 | 876.0334 | 0.2740 |

Figure 3). The blue circle represented targets of gastric cancer. The yellow circle represented targets of heat-clearing medicines. The orange circles represented targets of antirheumatic medicines. Among all the gastric cancer-relevant targets, 46 targets were the intersection of two types of medicines. A total of 44 targets were related to heat-
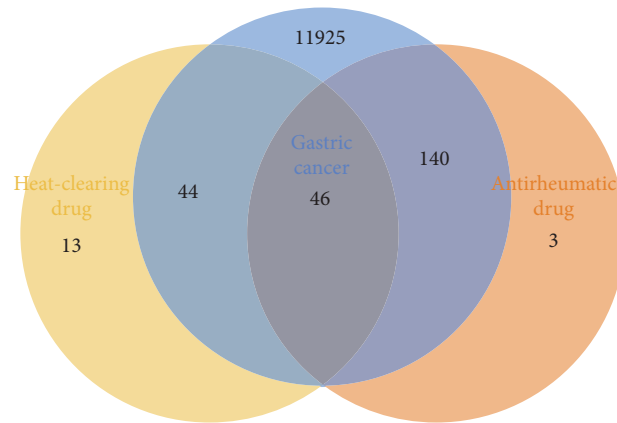
FIGURE 3: Venn diagram of relevant targets of medicines and gastric cancer. The blue, yellow, and orange circles denote targets of gastric cancer, heat-clearing medicines, and antirheumatic medicines, respectively.

clearing medicine, while 140 targets were related to antirheumatic medicines.

Based on coexpression analysis, gene detection, and gene interaction, the interactive targets were constructed into a PPI network (shown in Figure 4). The thickness of lines indicated the strength of data support from text mining, experiments, databases, coexpression, gene fusion, and cooccurrence. Targets of both medicines (Figure 4(a)) and targets of heat-clearing medicines (Figure 4(b)) constructed relatively simple networks. Targets of antirheumatic medicines constructed a quite complex network with lots of thick lines (Figure 4(c)). The area with thicker lines was considered as a module with higher biological significance, which needed further analysis based on the MCODE algorithm (shown in Figure 5 and Table 3). The MCODE algorithm was applied to identify neighborhoods where proteins were densely connected. Each MCODE network was assigned a unique color. As shown in Figure 5(a), four clusters were found in targets of antirheumatic medicines. Three clusters existed in targets of both medicines (Figure 5(b)). No cluster was found in targets of heat-clearing medicines.

*3.5. Enrichment Analysis and Visualization.* Enrichment analysis was performed based on the hypergeometric test and Benjamini-Hochberg $p$-value correction algorithm. The results of molecular function, biological process, cellular component, and KEGG pathway were visualized in a bubble chart using R software. As shown in Figure 6, antirheumatic medicine ranked the top in all the enrichment analyses. The top enrichment of biological processes included a response to lipopolysaccharide, response to molecule of bacterial origin, and response to the drug (Figure 6(a)). Enriched molecular functions mainly covered transcription factor binding, DNA-binding transcription factor binding, and RNA polymerase II-specific DNA-binding transcription factor binding (Figure 6(b)). Cellular components were mainly involved in the membrane microdomain and membrane raft (Figure 6(c)). As shown in Figure 6(d), both heat-clearing medicine and antirheumatic medicine were involved in pathways of cancer. Antirheumatic medicine had

a larger enrichment score. In the KEGG map of pathways in cancer (Figure 7), 65 targets of antirheumatic medicine were labeled green, 6 targets of heat-clearing medicine were marked red, and 6 targets relating to both medicines were in yellow. These targets took part in some important signaling pathways of cancer.

*3.6. Molecular Docking.* According to the result of MCODE algorithm (Table 3) and relevance score (Supplementary Table 2), the proteins with a high correlation with gastric cancer were selected for docking. The ligands were the ingredients related to the selected proteins (Supplementary Table 1).

After blind docking of ligands and proteins, we classified the docking results. It is generally considered that the lower affinity means a higher possibility of binding. The binding results are shown in Figure 8. The affinity is shown in Table 4. The binding affinity of AR and apigenin (ZINC3871576) was −8.48 kcal/mol. The active binding residues were GLN711, MET787, PHE764, and ASN705 (Figure 8(a)). MMP2 and luteolin (ZINC18185774) were bound with an affinity of −7.93 kcal/mol. The binding residues were THR143, ILE141, TYR3, PHE148, THR145, and ASN147(Figure 8(c)). The binding affinity of aloe-emodin (ZINC4098644) on TP53 was −6.08 kcal/mol. The binding residues were LYS24, PHE55, LEU54, and GLN59 (Figure 8(e)). Quercetin (ZINC3869685) could bind to AR, MMP2, TP53, and ERBB2. The binding of quercetin and AR was −7.82 kcal/mol. The active binding residues were GLN711, MET787, PHE764, LEU704, and LEU873 (Figure 8(b)). Quercetin and MMP2 were bound with an affinity of −7.90 kcal/mol. The binding residues were THR143, ILE141, TYR3, PHE148, THR145, and ASN147(Figure 8(d)). The binding affinity of quercetin on TP53 was −5.49 kcal/mol. The binding residues were PHE55 and LEU26(Figure 8(f)). Quercetin bound ERBB2 in residues of GLN1329, ASP1332, GLU1368, and PHE1306, with an affinity of −5.45 kcal/mol (Figure 8(g)). Among all the docking results, the binding of AR and apigenin had the lowest affinity, which meant that they were the most significant binding in this study.
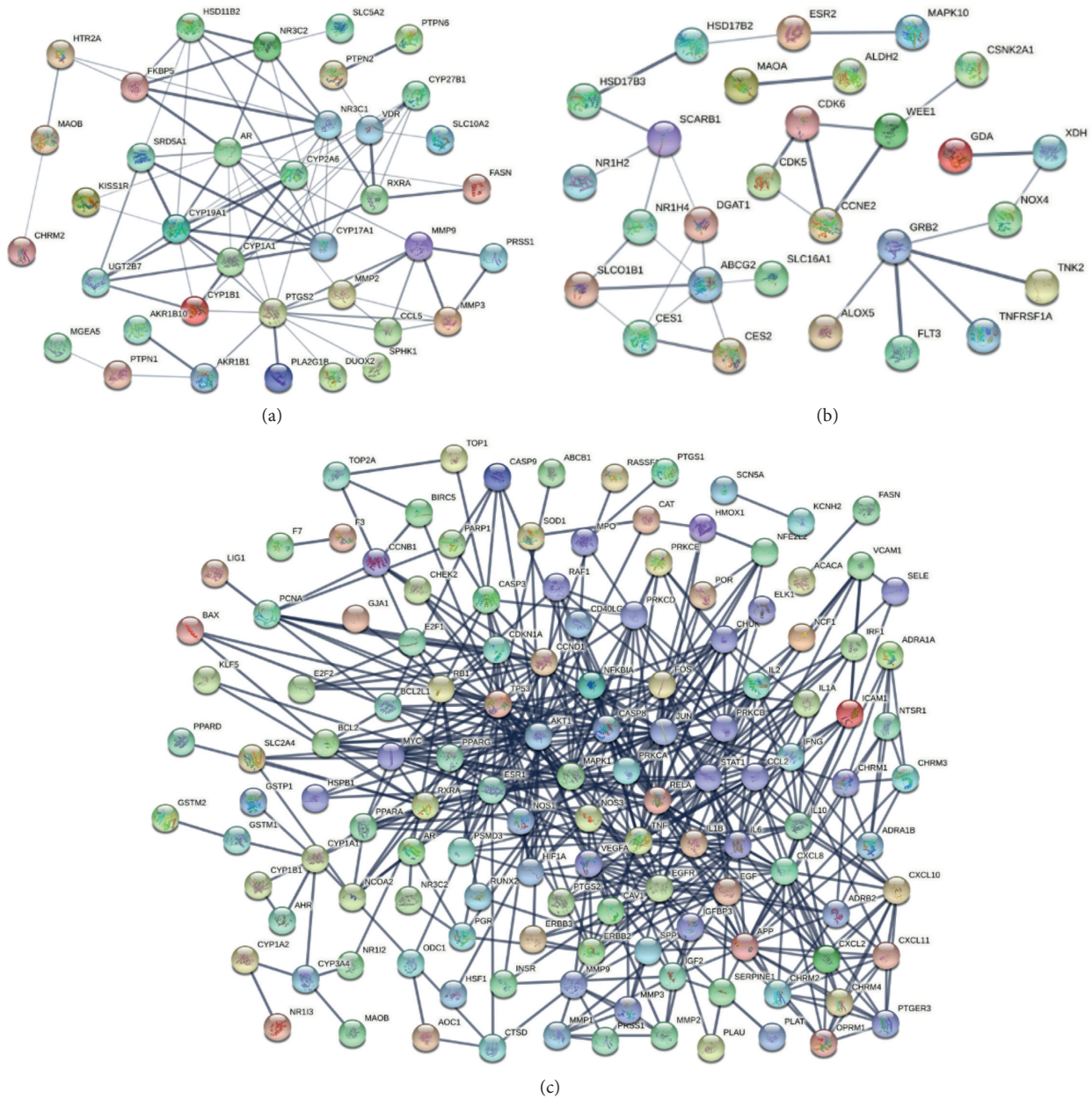
(a)

(b)

(c)

FIGURE 4: Protein-protein interaction network of coexpression genes: (a) genes expression in both types of medicines, (b) heat-clearing medicine, and (c) antirheumatic medicine. Each node representes a gene. Each line denotes the relationship between genes, and the thickness represents the strength of evidence.

*3.7. Analysis of Tumor Immune Infiltration.* Tumor immune infiltration is considered as a key factor of prognosis of tumor. We analyzed AR, MMP2, TP53, and ERBB2 in gastric tumor immune infiltration, and MMP2 and TP53 did not show significant result in this analysis. As shown in Figure 9(a), ERBB2 was negatively correlated with CD8+ T cell (partial.cor = −0.267, $p = 1.87E − 07$), macrophage (partial.cor = −0.309, $p = 1.33E − 09$), neutrophil (partial.cor = −0.291, $p = 1.15E − 08$), and dendritic cell (partial.cor = −0.325, $p = 1.39E − 10$). As shown in Figure 9(b), AR was positively correlated with CD4+ T cell (partial.cor = 0.484, $p = 6.21E − 23$), macrophage

(partial.cor = 0.618, $p = 2.44E − 40$), and dendritic cell (partial.cor = 0.352, $p = 3.06E − 12$).

sCNA was applied to compare immune infiltration distribution by the sCNA status of gene in STAD (abbreviations of stomach adenocarcinoma in TCGA cancer types). As shown in Table 5, high amplification of ERBB2 was in high correlation with six immune infiltrates ($p < 0.05$, Figure 10(a)). Arm-level deletion and gain of AR were significantly associated with CD8+ T cell, neutrophil, and dendritic cell ($p < 0.05$, Figure 10(b)).

Based on the TCGA database, the clinical outcome of gastric cancer was used to explore the relevance of tumor
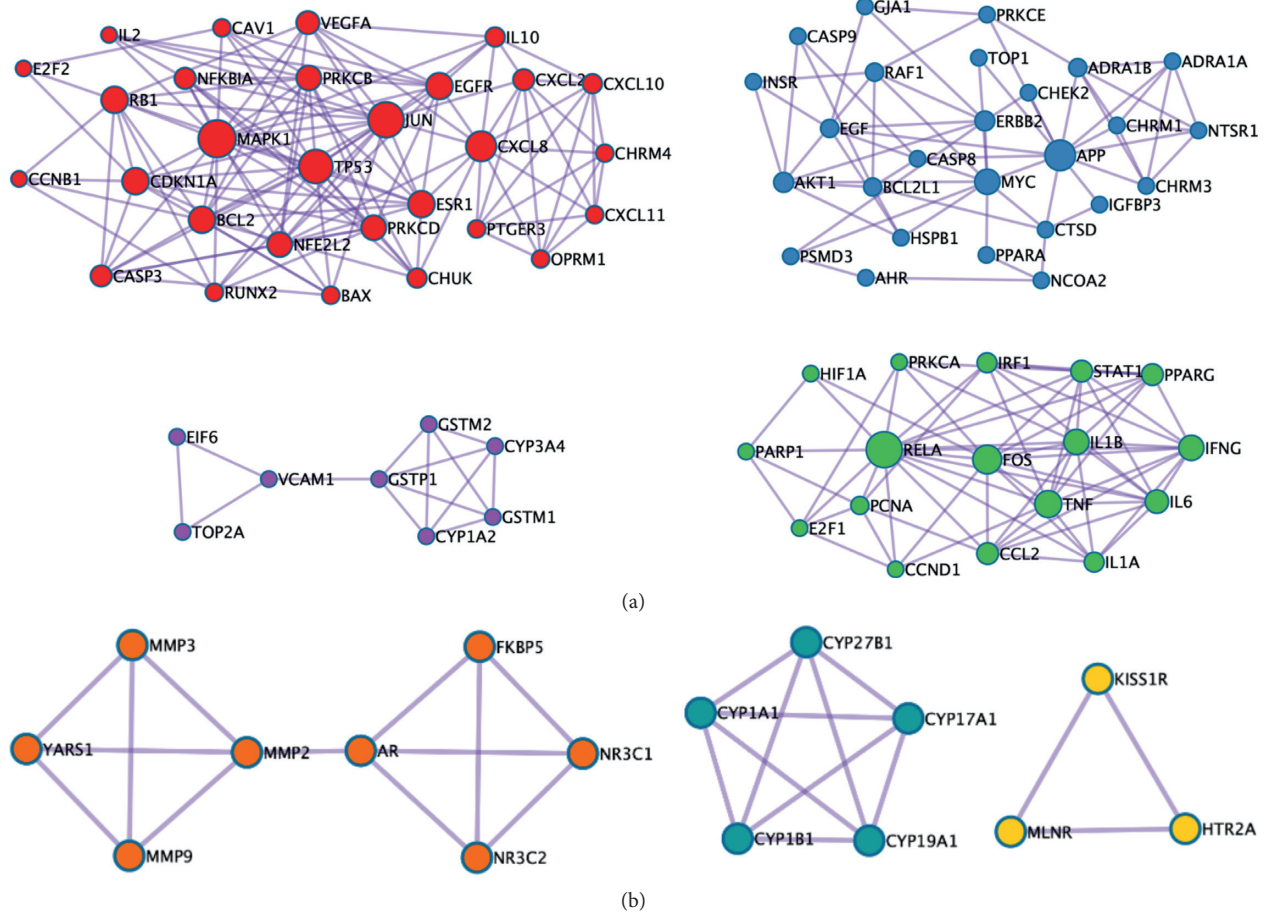
(a)



(b)

FIGURE 5: MCODE network of key targets. (a) 80 key targets of antirheumatic medicine were constructed in four MCODE networks. (b) 16 key targets of both types of medicines were constructed in three MCODE networks.

immune infiltration with multiple covariates in a multi-variable Cox proportional hazard model. The survival curves of gastric cancer showed a significant difference in macrophages at both 3-year time point (log-rank $p = 0.007$, Figure 11(a)) and 5-year time point (log-rank $p = 0.002$, Figure 11(b)).

## 4. Discussion

Heat-clearing medicine is a category of medicines that have the effect of clearing up internal heat in cases of externally contracted febrile diseases or fever due to yin deficiency. Tumor tissues are commonly in a state of rapid proliferation and high metabolism. The state is consistent with the feature of heat in TCM theory [59]. Based on this theory, several studies explored the mechanism of treating liver cancer, colon cancer, and lung cancer with heat-clearing medicine [60–65]. In clinical application, antirheumatic medicines are often used to treat tumors. HU Dan et al. found the ingredients and antitumor activity of *Tripterygii Radix* [66]. The chemical components of *Actinidia chinensis Planch* were extracted, and the antitumor effects were explored [67–69]. However, no study focused on the antitumor effects of the category of

antirheumatic medicine. Antirheumatic medicine is a category of medicine that dispels wind and dampness, mainly for relieving rheumatism and related conditions. Aiming to figure out the mechanism of treating gastric cancer with heat-clearing medicine and antirheumatic medicine, we searched relative ingredients and targets and constructed a network with gastric cancer-related targets. The result of enrichment analysis showed that two types of medicines were involved in pathways of cancer in different degrees of enrichment (Figure 6). All the relevant targets were marked in different colors in the KEGG map of pathways in cancer (Figure 7).

As shown in the KEGG map, testosterone and dihydrotestosterone are connected with androgen receptors (ARs) and expressed as the prostate-specific antigen (PSA). PSA had an indirect function in evading apoptosis (Figure 7). AR is a target closely related to two types of medicine and gastric cancer (relevant score = 54.93). AR is related to two ingredients, namely, apigenin and quercetin. Molecular docking was performed to verify the binding ability of AR and ingredients. The binding strength of AR and apigenin was the strongest among all the bindings in this study (Table 4). AR and quercetin were bounded with a weaker affinity. The result showed that the antitumor effects

TABLE 3: The parameter of the MCODE network.

| | Score | Gene | Symbol | Network |
|---|---|---|---|---|
| Clusters for both types of medicines | 1.25 | 1588 | CYP19A1 | MyList_SUB1 |
| | 1.25 | 6715 | SRD5A1 | MyList_SUB1 |
| | 1.25 | 7364 | UGT2B7 | MyList_SUB1 |
| | 1.25 | 1586 | CYP17A1 | MyList_SUB1 |
| | 1 | 3356 | HTR2A | MyList_SUB2 |
| | 1 | 2862 | MLNR | MyList_SUB2 |
| | 1 | 84634 | KISS1R | MyList_SUB2 |
| Clusters for heat-clearing medicine | 1.79999999999999 | 5644 | PRSS1 | MyList_SUB1 |
| | 1.79999999999999 | 4322 | MMP13 | MyList_SUB1 |
| | 1.79999999999999 | 4314 | MMP3 | MyList_SUB1 |
| | 1.79999999999999 | 4318 | MMP9 | MyList_SUB1 |
| | **1.79999999999999** | **4313** | **MMP2** | **Mylist_SUB1** |
| | 1 | 217 | ALDH2 | MyList_SUB2 |
| | 1 | 4128 | MAOA | MyList_SUB2 |
| | 1 | 4129 | MAOB | MyList_SUB2 |
| Clusters for antirheumatic medicine | 6.5 | 1869 | E2F1 | MyList_SUB2 |
| | 6.5 | 3725 | JUN | MyList_SUB2 |
| | **6.5** | **7157** | **TP53** | **Mylist_SUB2** |
| | 6.5 | 3659 | IRF1 | MyList_SUB2 |
| | 6.5 | 581 | BAX | MyList_SUB2 |
| | 6.5 | 3576 | CXCL8 | MyList_SUB2 |
| | 6.5 | 5111 | PCNA | MyList_SUB2 |
| | 6.5 | 595 | CCND1 | MyList_SUB2 |
| | 6.5 | 4609 | MYC | MyList_SUB2 |
| | 6.5 | 5594 | MAPK1 | MyList_SUB2 |
| | 6.5 | 5970 | RELA | MyList_SUB2 |
| | 6.5 | 1147 | CHUK | MyList_SUB2 |
| | 6.5 | 4318 | MMP9 | MyList_SUB2 |
| | 6.5 | 5925 | RB1 | MyList_SUB2 |
| | 6.5 | 207 | AKT1 | MyList_SUB2 |
| | 6.5 | 1956 | EGFR | MyList_SUB2 |
| | 6.5 | 2099 | ESR1 | MyList_SUB2 |
| | 6.5 | 3091 | HIF1A | MyList_SUB2 |
| | 6.5 | 860 | RUNX2 | MyList_SUB2 |
| | 6.5 | 142 | PARP1 | MyList_SUB2 |
| | 6.5 | 5578 | PRKCA | MyList_SUB2 |
| | 6.5 | 3558 | IL2 | MyList_SUB2 |
| | 6.5 | 2353 | FOS | MyList_SUB2 |
| | **6.5** | **367** | **AR** | **MyList_SUB2** |
| | 3.375 | 6347 | CCL2 | MyList_SUB4 |
| | 3.375 | 3586 | IL10 | MyList_SUB4 |
| | 3.375 | 5743 | PTGS2 | MyList_SUB4 |
| | 3.375 | 5733 | PTGER3 | MyList_SUB4 |
| | 3.375 | 6373 | CXCL11 | MyList_SUB4 |
| | 3.375 | 1132 | CHRM4 | MyList_SUB4 |
| | 3.375 | 3553 | IL1B | MyList_SUB4 |
| | 3.375 | 3552 | IL1A | MyList_SUB4 |
| | 3.375 | 1129 | CHRM2 | MyList_SUB4 |
| | 3.375 | 4988 | OPRM1 | MyList_SUB4 |
| | 3.375 | 2920 | CXCL2 | MyList_SUB4 |
| | 3.375 | 3458 | IFNG | MyList_SUB4 |
| | 3.375 | 3569 | IL6 | MyList_SUB4 |
| | 3.375 | 3627 | CXCL10 | MyList_SUB4 |
| | 3.375 | 5468 | PPARG | MyList_SUB4 |
| | 3.375 | 6772 | STAT1 | MyList_SUB4 |
| | 3.03125 | 5709 | PSMD3 | MyList_SUB1 |
| | 3.03125 | 1576 | CYP3A4 | MyList_SUB1 |
| | 3.03125 | 3383 | ICAM1 | MyList_SUB1 |
| | 3.03125 | 1544 | CYP1A2 | MyList_SUB1 |
| | 3.03125 | 1543 | CYP1A1 | MyList_SUB1 |
| | 3.03125 | 7124 | TNF | MyList_SUB1 |
| | 3.03125 | 2950 | GSTP1 | MyList_SUB1 |
| | 3.03125 | 3486 | IGFBP3 | MyList_SUB1 |
| | 3.03125 | 836 | CASP3 | MyList_SUB1 |
| | 3.03125 | 5465 | PPARA | MyList_SUB1 |
| | 3.03125 | 596 | BCL2 | MyList_SUB1 |
| | 3.03125 | 10499 | NCOA2 | MyList_SUB1 |
| | 3.03125 | 891 | CCNB1 | MyList_SUB1 |
| | 3.03125 | 5580 | PRKCD | MyList_SUB1 |
| | 3.03125 | 1545 | CYP1B1 | MyList_SUB1 |
| | 3.03125 | 4846 | NOS3 | MyList_SUB1 |
| | 3.03125 | 1870 | E2F2 | MyList_SUB1 |
| | 3.03125 | 1026 | CDKN1A | MyList_SUB1 |
| | 3.03125 | 1950 | EGF | MyList_SUB1 |
| | 3.03125 | 5579 | PRKCB | MyList_SUB1 |
| | 3.03125 | 857 | CAV1 | MyList_SUB1 |
| | 3.03125 | 7422 | VEGFA | MyList_SUB1 |
| | 3.03125 | 5241 | PGR | MyList_SUB1 |
| | 3.03125 | 196 | AHR | MyList_SUB1 |
| | 3.03125 | 2946 | GSTM2 | MyList_SUB1 |
| | 3.03125 | 2944 | GSTM1 | MyList_SUB1 |
| | 3.03125 | 11200 | CHEK2 | MyList_SUB1 |
| | 3.03125 | 4312 | MMP1 | MyList_SUB1 |
| | 3.03125 | 3315 | HSPB1 | MyList_SUB1 |
| | 3.03125 | 6256 | RXRA | MyList_SUB1 |
| | 3.03125 | 5894 | RAF1 | MyList_SUB1 |
| | 3.03125 | 4792 | NFKBIA | MyList_SUB1 |
| | 1.85 | 147 | ADRA1B | MyList_SUB3 |
| | 1.85 | 7153 | TOP2A | MyList_SUB3 |
| | 1.85 | 653361 | NCF1 | MyList_SUB3 |
| | 1.85 | 7412 | VCAM1 | MyList_SUB3 |
| | 1.85 | 5581 | PRKCE | MyList_SUB3 |
| | 1.85 | 4780 | NFE2L2 | MyList_SUB3 |
| | 1.85 | 598 | BCL2L1 | MyList_SUB3 |
| | 1.85 | 148 | ADRA1A | MyList_SUB3 |
| | **1.85** | **4313** | **MMP2** | **Mylist_SUB3** |
| | 1.85 | 4923 | NTSR1 | MyList_SUB3 |
| | 1.85 | 841 | CASP8 | MyList_SUB3 |
| | 1.85 | 959 | CD40LG | MyList_SUB3 |
| | 1.85 | 351 | APP | MyList_SUB3 |
| | 1.85 | 1509 | CTSD | MyList_SUB3 |
| | 1.85 | 3481 | IGF2 | MyList_SUB3 |
| | 1.85 | 2065 | ERBB3 | MyList_SUB3 |
| | **1.85** | **2064** | **ERBB2** | **MyList_SUB3** |
| | 1.85 | 1128 | CHRM1 | MyList_SUB3 |
| | 1.85 | 1131 | CHRM3 | MyList_SUB3 |
| | 1.85 | 7150 | TOP1 | MyList_SUB3 |

Bold represents the targets with high relevance score and selected for docking.
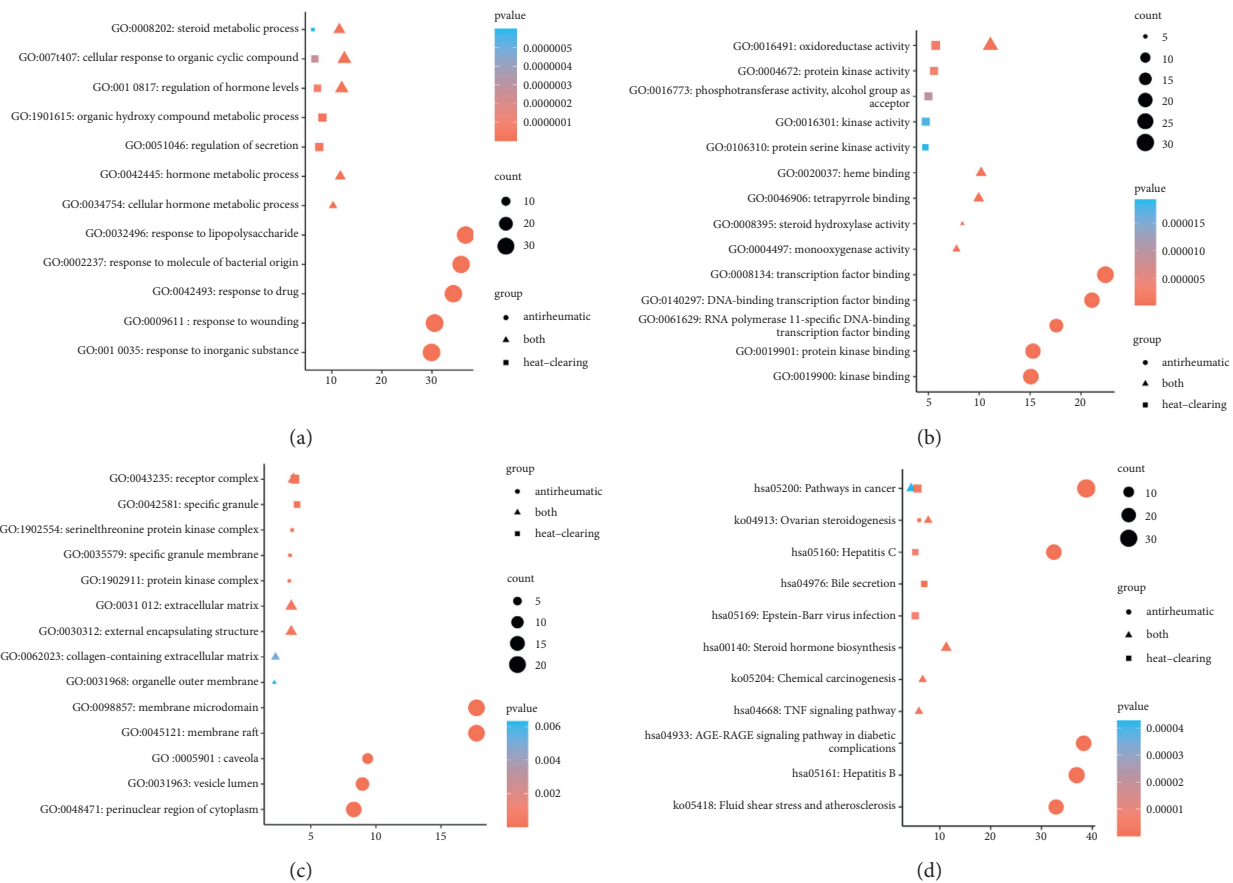
Figure 6: GO and KEGG enrichment analysis: (a) the top enriched pathways of biological process, (b) molecular function, (c) cellular component, and (d) KEGG pathway. The circles, squares, and triangles denote antirheumatic medicine, heat-clearing medicine, and both types of medicine. The node size represents a degree of enrichment. Red color represents more significance of enrichment.

of both heat-clearing medicine and antirheumatic medicine were closely related to androgen action.

In the KEGG map of pathways in cancer, matrix metalloproteinases (MMPs) were involved in process of sustained angiogenesis (Figure 7). It is generally accepted that the mechanism of MMPs is mostly related to matrix reconstruction, including decomposition of extracellular matrix proteins and cell surface receptors in cancer proliferation [70]. MMP9 and MMP2 are gelatinases, a subtype of matrix metalloproteinases (MMPs). The levels of serum MMP9 and MMP2 in patients with gastric cancer were significantly higher than normal people in clinical practice [71]. MMP9 and MMP2 accelerate tumor metastasis by invading lymphatic vessels and small vessels [72, 73]. On one hand, helicobacter pylori infection might enhance the expression of MMPs, induce cell proliferation, and activate gene oncogenes [74, 75]. On the other hand, MMP9 and MMP2 could degrade type IV collagen in the extracellular matrix and basement membranes. This process plays an important role in tumor invasion and metastasis [76–79]. In this study, the results of MCODE analysis indicated that MMP9 and MMP2 were key targets in the antitumor function of both heat-clearing medicine and antirheumatic medicine. In molecular docking experiments, MMP2 bounded luteolin and quercetin with low binding energy

(Table 4). However, MMP9 failed to bind any related ingredients of heat-clearing medicine and antirheumatic medicine.

Based on the p53 signaling pathway in the KEGG map (Figure 7), tumor protein p53 missed the interaction with cyclin-dependent kinase inhibitor 1A(p21). p21 is a mediator of p53 tumor suppressor activity based on functions of growth arresting, differentiation, and senescence [80]. p21 inhibits the complex formation of cyclin-dependent kinase 4/6(CDK4/6) and G1/S-specific cyclin D1(CyclinD) [80]. CDK4/6 plays a key role in cell cycle regulation. After phosphorylation, transcription factor E2F1(E2F) dissociates from retinoblastoma-associated protein (Rb) and expresses as proliferation [81]. To predict the interaction of TP53 and related ingredients of antirheumatic medicine, we performed molecular docking experiments. The binding strength of TP53 and aloe-emodin, TP53, and quercetin was moderate (Table 4). The results revealed that antirheumatic medicine was in closed relation to the p53 signaling pathway.

In the KEGG pathway map, epidermal growth factor (EGF) interacts with epidermal growth factor receptor (EGFR) and receptor tyrosine-protein kinase erbB-2 (ERBB2) (Figure 7). Both EGFR and ERBB2 are receptor protein-tyrosine kinases with a transmembrane domain [82]. These receptors have two ways of activation. One way is
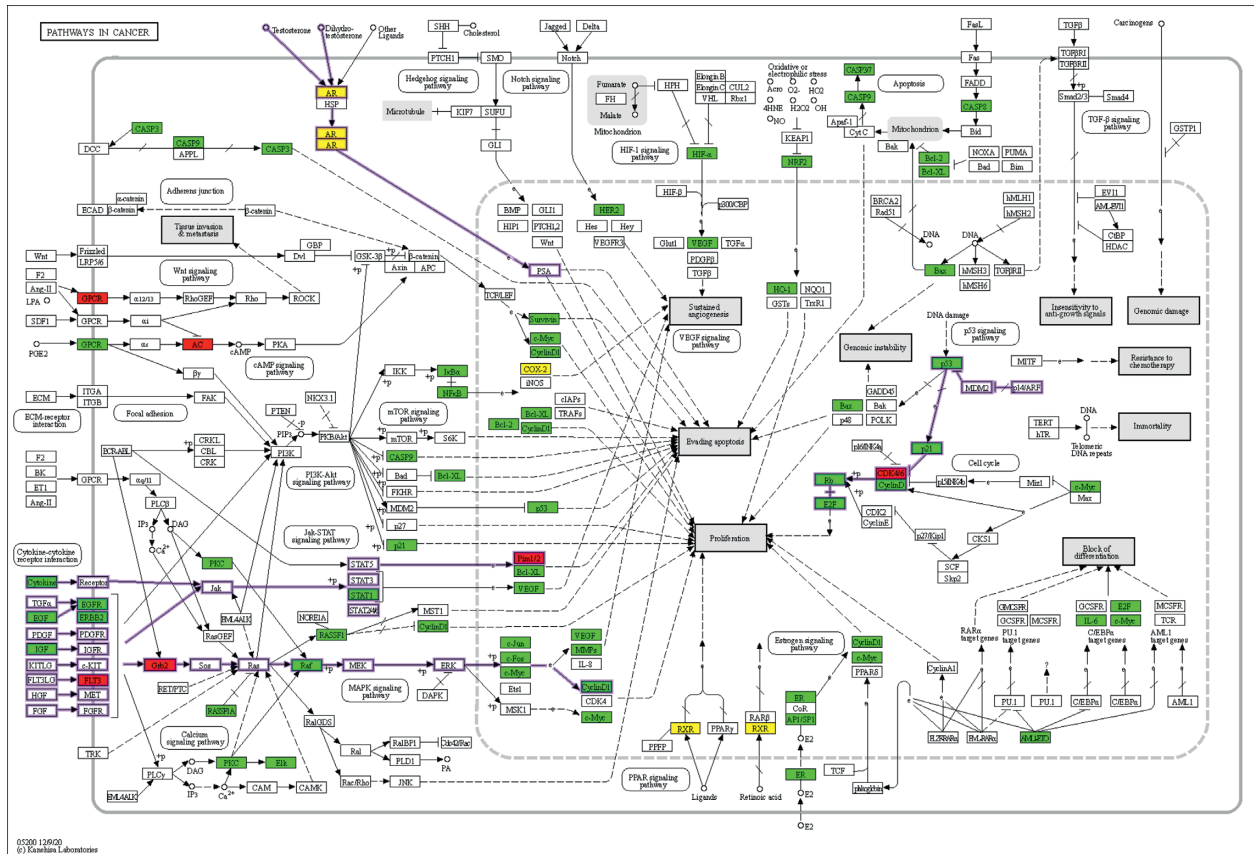
Figure 7: KEGG map of pathways in cancer. The red rectangles represent 6 proteins relevant to heat-clearing medicine. The green rectangles represent 65 proteins of antirheumatic medicine. Six yellow rectangles represent the protein relevant to both types of medicines.
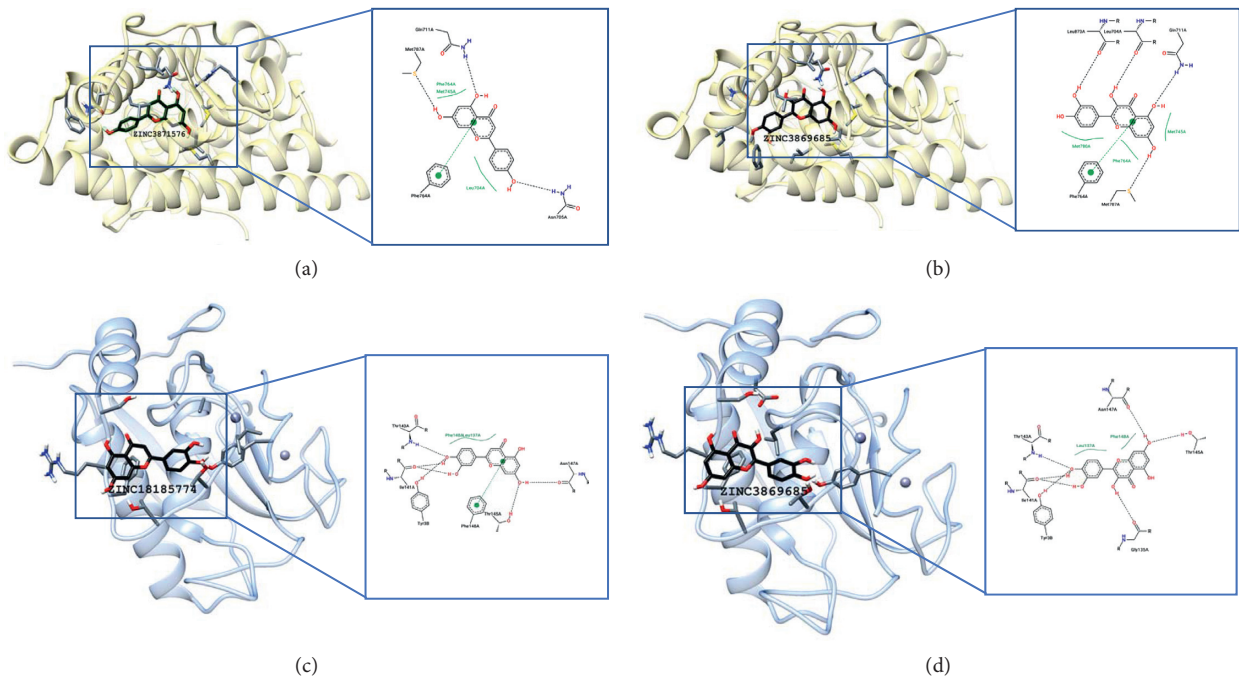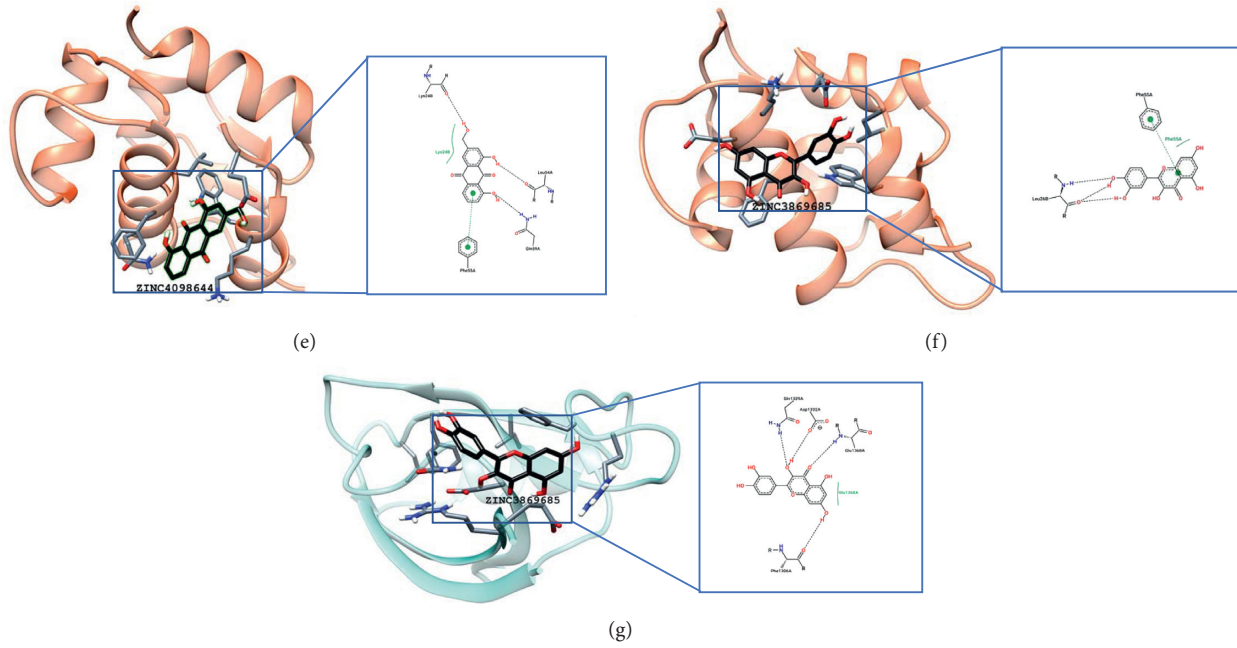


(a)



(b)



(c)



(d)

Figure 8: Continued.

(e)

(f)

(g)

FIGURE 8: Molecular docking of key targets and ligands. (a) AR and apigenin. (b) AR and quercetin. (c) MMP2 and luteolin. (d) MMP2 and quercetin. (e) TP53 and aloe-emodin. (f) TP53 and quercetin. (g) ERBB2 and quercetin. The ribbons represent the targets, the black sticks represent the ligands, and the gray sticks represent the intermolecular bonding.

TABLE 4: The result of molecular docking.

|  | Target | Ligand | Binding energy (kcal/mol) | Binding residues |  |
| --- | --- | --- | --- | --- | --- |
| (a) | AR | Apigenin (ZINC3871576) | −8.48 | GLN711, MET787, PHE764, ASN705 | 15 |
| (b) | AR | Quercetin (ZINC3869685) | −7.82 | GLN711, MET787, PHE764, LEU704, LEU873 | 18 |
| (c) | MMP2 | Luteolin (ZINC18185774) | −7.93 | THR143, ILE141, TYR3, PHE148, THR145, ASN147 | 56 |
| (d) | MMP2 | Quercetin (ZINC3869685) | −7.90 | THR143, ILE141, TYR3, GLY135, THR145, ASN147 | 58 |
| (e) | TP53 | Aloe-emodin (ZINC4098644) | −6.08 | LYS24, PHE55, LEU54, GLN59 | 37 |
| (f) | TP53 | Quercetin (ZINC3869685) | −5.49 | PHE55, LEU26 | 38 |
| (g) | ERBB2 | Quercetin (ZINC3869685) | −5.45 | GLN1329, ASP1332, GLU1368, PHE1306 | 48 |



(a)

(b)
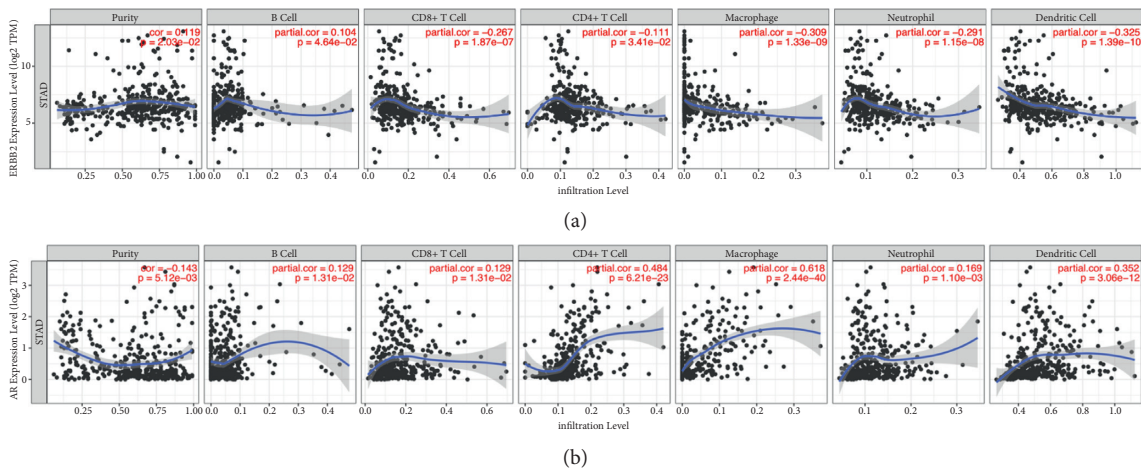
FIGURE 9: The correlation between gene expression and abundances of six immune infiltrates in gastric cancer: (a) ERBB2, and (b) AR.

TABLE 5: The correlation between immune infiltrates and somatic copy number alterations.

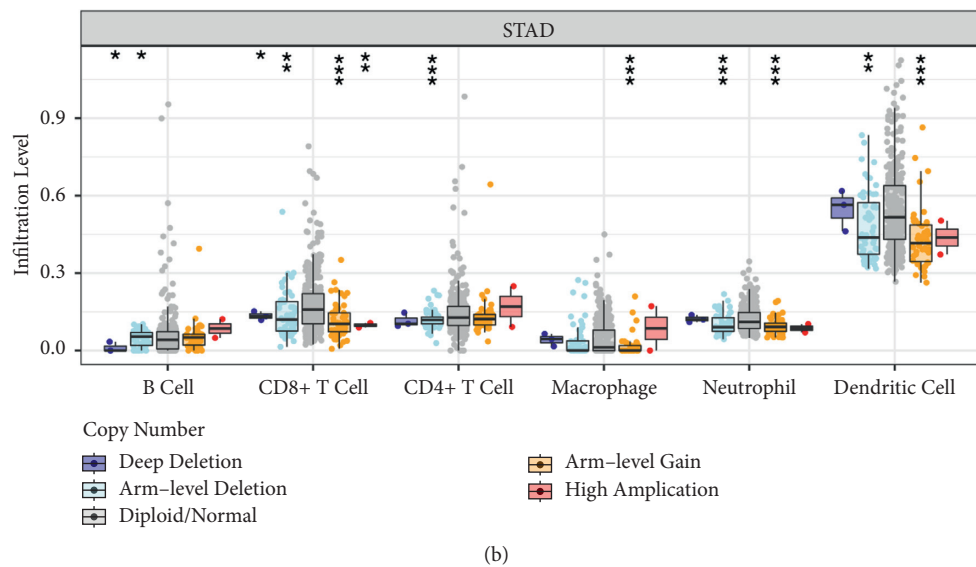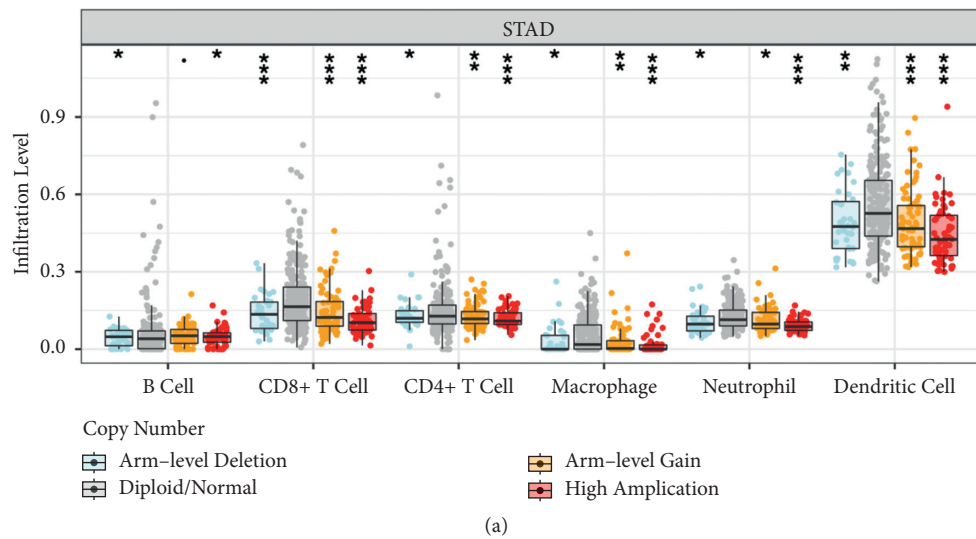| | ERBB2 | | | | |
| --- | --- | --- | --- | --- | --- |
| | Arm-level deletion | Diploid/normal | Arm-level gain | High amplification | |
| B cell | $2.74E - 02$ | $1.00E + 00$ | $9.51E - 02$ | $4.20E - 02$ | |
| CD8+ T cell | $4.08E - 04$ | $1.00E + 00$ | $2.66E - 04$ | $4.21E - 13$ | |
| CD4+ T cell | $2.70E - 02$ | $1.00E + 00$ | $7.32E - 03$ | $7.90E - 05$ | |
| Macrophage | $4.45E - 02$ | $1.00E + 00$ | $2.30E - 03$ | $8.61E - 07$ | |
| Neutrophil | $2.03E - 02$ | $1.00E + 00$ | $1.38E - 02$ | $2.22E - 12$ | |
| Dendritic cell | $1.73E - 03$ | $1.00E + 00$ | $1.42E - 04$ | $3.89E - 09$ | |
| | AR | | | | |
| | Arm-level deletion | Diploid/normal | Arm-level gain | High amplification | Deep deletion |
| B cell | $3.91E - 02$ | $1.00E + 00$ | $3.78E - 01$ | $6.37E - 01$ | $2.44E - 02$ |
| CD8+ T cell | $2.32E - 03$ | $1.00E + 00$ | $3.69E - 07$ | $7.58E - 03$ | $1.03E - 02$ |
| CD4+ T cell | $6.56E - 04$ | $1.00E + 00$ | $2.59E - 01$ | $8.27E - 01$ | $1.60E - 01$ |
| Macrophage | $3.20E - 01$ | $1.00E+00$ | $4.75E - 05$ | $7.40E - 01$ | $6.74E - 01$ |
| Neutrophil | $9.78E - 04$ | $1.00E + 00$ | $1.26E - 06$ | $2.53E - 01$ | $9.48E - 01$ |
| Dendritic cell | $1.19E - 03$ | $1.00E + 00$ | $9.62E - 08$ | $3.30E - 01$ | $9.63E - 01$ |



(a)



(b)

FIGURE 10: The correlation between immune infiltrates and somatic copy number alterations (SCNAs) of gene expression of gastric cancer: (a) ERBB2, and (b) AR.
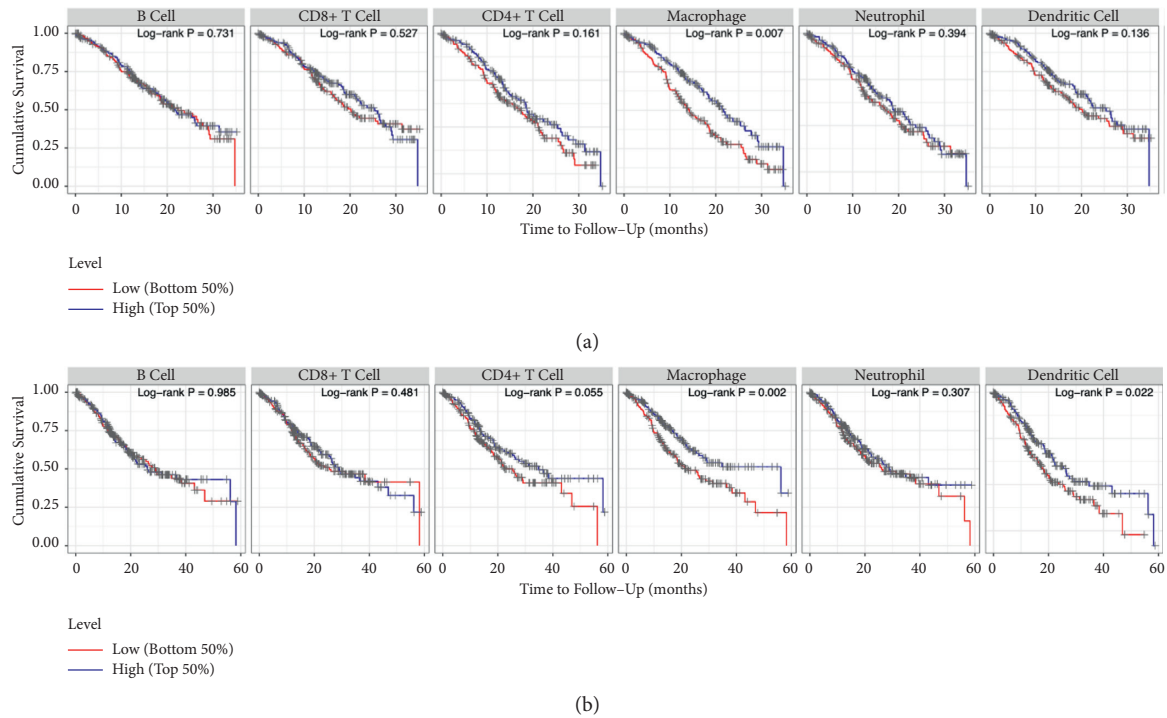
FIGURE 11: The survival curves of gastric cancer and abundance of immune infiltrate: (a) 3-year time point and (b) 5-year time point.

activating with growth factor receptor-bound protein 2(Grb2) in the MAPK signaling pathway [83, 84]. The other way is activating with Janus kinase 1(Jak) and phosphorylated as an activator of transcription 1 (STAT1). STAT1 is expressed as a vascular endothelial growth factor (VEGF), with an indirect function of sustained angiogenesis [85]. The pathway of proliferation and sustained angiogenesis mainly happened with antirheumatic medicine. Aiming to testify the binding ability of ERBB2 and its related ingredients, molecular docking experiments were performed. The result showed that the binding strength of ERBB2 and quercetin was moderate (Table 4).

Summarizing the docking results above, quercetin could bind several gastric cancer-related targets. Quercetin existed in both types of medicines. It is an important ingredient in both heat-clearing medicine and antirheumatic medicine. Previous studies showed that quercetin was effective in treating gastric cancer. In a scratch wound healing assay, Jia et al. [86] found that the TGF$\beta$-1 and quercetin group had worse proliferation capability and migration ability of human gastric carcinoma BGC-803 cells. It revealed that quercetin can effectively inhibit the metastasis and invasion of gastric cancer. Yu. [87] treated gastric cancer MGC-803 cells with quercetin for 48 hours and found that quercetin could decrease the expression of VEGF-C and VEGFR-3. This process is involved in inhibiting gastric cancer proliferation and lymph node metastasis. MC Kim et al. [88] found that quercetin could inhibit mitogen-activated protein kinases (MAPKs) and accelerate apoptosis of AGS cells in gastric cancer.

Based on the theory of tumor microenvironment and antitumor immunity, we analyze the tumor immune infiltration of the key proteins in this study to explore the immune response in tumor tissue. The result of tumor immune infiltration showed that AR was positively correlated with CD4+ T cells, macrophages, and dendritic cells, while ERBB2 was negatively correlated with CD8+ T cells, macrophages, neutrophils, and dendritic cells (Figure 9). However, TP53 and MMP2 showed no significant correlation in tumor immune infiltration analysis. The result revealed that the tumor immune infiltration was different in AR and ERBB2 expression. If the expression of ERBB2 increased, the relevant immune cells decreased. If the expression of AR increased, the relevant immune cells increased.

Combining the results of enrichment analysis and tumor immune infiltration analysis, the pathway of androgen was correlated with both heat-clearing medicine and antirheumatic medicine in treating gastric cancer. There are some possible reasons. First, the incidence of male and female patients with gastric cancer is approximately in the ratio 2 : 1 (estimated number of new gastric cancer in age-standardized rates per ten thousand: men = 15.8, women = 7.0 [1]). A prospective cohort study on upper gastrointestinal cancers and hormonal and reproductive factors showed that male pattern baldness was associated with gastric cancer risk in an adjusted hazard ratio of 1.35 [89]. The evidence above revealed a close association with gastric cancer and sex hormones, especially androgen. Second, men prefer food with stronger flavors, such as barbecue, red meat, and alcohol. Heavy meal combining with yang excessiveness constitution generally leads to heat syndrome. Third, androgens can reduce antibody production and suppress the immune system. Clinically, men are less likely to develop

autoimmune diseases than women do [90, 91]. AR signaling has been proved to have a direct or indirect influence on immune cell function. Above all, AR is an important target in both heat-clearing medicine and antirheumatic medicine. Male patients or female patients with androgen excess are more likely to activate AR signaling pathway. Further searches on gastric cancer of sex hormones are required.

In tumor progression, ERBB2 interacts with epidermal growth factor receptors (EGFRs) and activates signaling pathways of tumor proliferation. ERBB2 plays a role in tumor cells by binding to other epidermal growth factor receptors (EGFRs) and then generating a dimer form that activates signaling pathways related to tumor proliferation [92–95]. Trastuzumab is a monoclonal antibody targeting the extracellular region IV of ERBB2. As a targeted drug for gastric cancer, trastuzumab could stop the formation of ERBB2 homologous dimers, prevent the activation of the signaling pathways of cell proliferation, and kill tumor cells through antibody-dependent cellular cytotoxicity [94]. Pertuzumab is another targeted drug for gastric cancer based on ERBB2. It shows positive efficacy in patients with advanced gastric cancer with high expression of ERBB2. In this study, antirheumatic medicine had a similar pathway to trastuzumab and pertuzumab [96]. It inferred that antirheumatic medicine could stop the formation of ERBB2 homologous dimers, prevent cell proliferation, and kill tumor cells. Further research for dose-response analysis and compatibility of drugs is needed.

The results of gastric cancer survival curves showed that macrophage was significantly different at both the 3-year time point and 5-year time point (Figure 11). It revealed that the number of macrophages might influence gastric cancer prognosis. Previous studies found that macrophages are important components of tumor inflammatory infiltrating cells [97–99]. M1 subtype promotes antitumor immunity, while the M2 subtype is associated with tumor progression. The research found that high density of M2 tumor-associated macrophages (TAMs) was correlated with poor disease-free survival and cancer-specific survival [100]. Intraperitoneal TAMs were generally polarized to the M2 phenotype in patients with gastric cancer with peritoneal dissemination [101]. Infiltration of polarized TAMs combined with the TNM stage could be prognostic factors for gastric cancer [102].

This study creatively combined network pharmacology and molecular docking with tumor immune infiltration analysis to explore the pharmacological mechanism of treating gastric cancer with heat-clearing medicine and antirheumatic medicine. Not only the relationship of ingredients and targets were investigated but also the tumor immune infiltration was analyzed. It is a new way to explore TCM in tumor immunology. Here are some limitations of this study. First, the ingredients of medicines are currently not comprehensive. It might lead to some deviation. Further research on the ingredients of herbal medicines is needed. Second, molecular docking experiments were performed to verify the binding of targets and ligands, but the result was based on molecular simulation. Extra in vitro experiments,

animal studies, and clinical trials are required to validate the inference.

In conclusion, quercetin is an important ingredient in both heat-clearing medicine and antirheumatic medicine. AR signaling pathway exists in both types of medicines. The mechanism of antitumor effect in antirheumatic medicine was similar to trastuzumab, a targeted drug aimed at ERBB2. Both types of medicines were significant in tumor immune infiltration. The immunology of gastric tumor deserves further research.

## Data Availability

The data can be found in the database, including TCMSP database (https://old.tcmsp-e.com/tcmsp.php), CancerHSP database (https://old.tcmsp-e.com/CancerHSP.php), Uni-Prot protein database (https://www.uniprot.org), Gene-Cards database (https://www.genecards.org), OMIM database (https://www.omim.org), TTD database (https://bidd.nus.edu.sg/group/cjttd), and DrugBank database (https://www.drugbank.ca).

## Conflicts of Interest

The authors declare that they have no conflicts of interest with other people or organizations that can inappropriately influence our work, and there is no professional or other personal interest of any nature or kind in any product, service, and/or company that could be construed as influencing the position presented in, or the review of, the manuscript entitled, comparison between heat-clearing medicine and antirheumatic medicine in the treatment of gastric cancer based on network pharmacology, molecular docking, and tumor immune infiltration analysis.

## Authors' Contributions

Jiamin Xu drafted the manuscript and analyzed the data. Wei Wang and Fuqin Kang operated the molecular docking and revised the manuscript. Shujun Liu collected the data. Jianhui Xie interpreted the data. Xiaobo Yang conceived and designed the project and acquired funding. All authors read and approved the final manuscript.

## Acknowledgments

## Supplementary Materials

Supplementary Table 1: The relevant targets of medicines. Supplementary Table 2: Gastric cancer-related targets and relevance score. (*Supplementary Materials*)

## References

[1] Lyon, France: international agency for research on cancer [EB/OL], [2020-11-20], https://gco.iarc.fr/today/online-analysis-table.

[2] F. H. Wang, X. T. Zhang, Y. F. Li et al., "The Chinese Society of Clinical Oncology (CSCO): clinical guidelines for the diagnosis and treatment of gastric cancer, 2021," *Cancer Communications*, vol. 41, no. 8, pp. 747–795, 2021.

[3] J.-B. Hu, X.-N. Sun, B.-X. Gu, Q. Wang, and W.-X. Hu, "Effect of intensity modulated radiotherapy combined with s-1-based chemotherapy in locally advanced gastric cancer patients," *Oncology Research and Treatment*, vol. 37, no. 1-2, pp. 11–16, 2014.

[4] J. Lee, D. H. Lim, S. Kim et al., "Phase III trial comparing capecitabine plus cisplatin versus capecitabine plus cisplatin with concurrent capecitabine radiotherapy in completely resected gastric cancer with D2 lymph node dissection: the ARTIST trial," *Journal of Clinical Oncology*, vol. 30, no. 3, pp. 268–273, 2012.

[5] T. Inoue, S. Yachida, H. Usuki et al., "Pilot feasibility study of neoadjuvant chemoradiotherapy with S-1 in patients with locally advanced gastric cancer featuring adjacent tissue invasion or JGCA bulky N2 lymph node metastases," *Annals of Surgical Oncology*, vol. 19, no. 9, pp. 2937–2945, 2012.

[6] X. Wang, D. B. Zhao, L. Yang et al., "S-1 chemotherapy and intensity-modulated radiotherapy after D1/D2 lymph node dissection in patients with node-positive gastric cancer: a phase I/II study," *British Journal of Cancer*, vol. 118, no. 3, pp. 338–343, 2018.

[7] Y. Liu, G. Zhao, Y. Xu et al., "Multicenter phase 2 study of peri-irradiation chemotherapy plus intensity modulated radiation therapy with concurrent weekly docetaxel for inoperable or medically unresectable nonmetastatic gastric cancer," *International Journal of Radiation Oncology, Biology, Physics*, vol. 98, no. 5, pp. 1096–1105, 2017.

[8] J. Wang, R. Xu, J. Li et al., "Randomized multicenter phase III study of a modified docetaxel and cisplatin plus fluorouracil regimen compared with cisplatin and fluorouracil as first-line therapy for advanced or locally recurrent gastric cancer," *Gastric Cancer*, vol. 19, no. 1, pp. 234–244, 2016.

[9] Y. Yamada, N. Boku, J. Mizusawa et al., "Docetaxel plus cisplatin and S-1 versus cisplatin and S-1 in patients with advanced gastric cancer (JCOG1013): an open-label, phase 3, randomised controlled trial," *The Lancet Gastroenterology & Hepatology*, vol. 4, no. 7, pp. 501–510, 2019.

[10] H. Ishigami, Y. Fujiwara, R. Fukushima et al., "Phase III trial comparing intraperitoneal and intravenous paclitaxel plus S-1 versus cisplatin plus S-1 in patients with gastric cancer with peritoneal metastasis: PHOENIX-GC trial," *Journal of Clinical Oncology*, vol. 36, no. 19, pp. 1922–1929, 2018.

[11] K. Shitara, A. Takashima, K. Fujitani et al., "Nab-paclitaxel versus solvent-based paclitaxel in patients with previously treated advanced gastric cancer (ABSOLUTE): an open-label, randomised, non-inferiority, phase 3 trial," *The Lancet Gastroenterology & Hepatology*, vol. 2, no. 4, pp. 277–287, 2017.

[12] Q. Li, H. Jiang, H. Li et al., "Efficacy of trastuzumab beyond progression in HER2 positive advanced gastric cancer: a multicenter prospective observational cohort study," *Oncotarget*, vol. 7, no. 31, pp. 50656–50665, 2016.

[13] K. Shitara, M. Özgüroğlu, Y. J. Bang et al., "KEYNOTE-061 investigators. Pembrolizumab versus paclitaxel for previously treated, advanced gastric or gastro-oesophageal junction cancer (KEYNOTE-061): a randomised, open-label, controlled, phase 3 trial," *Lancet*, vol. 392, no. 10142, pp. 123–133, 2018.

[14] D. Y. Ma and M. Liu, "Effect of Yiqi Qingrejiudu prescription combined with chemotherapy on peripheral blood Th17Treg cell balance and quality of life in patients with advanced gastric cancer," *Sichuan Traditional Chinese Medicine*, vol. 36, no. 8, pp. 83–87, 2018.

[15] S. B. Ma, D. D. Lin, and H. Y. Liu, "The role of inflammatory cytokines in tumor microenvironment and their therapeutic targets," *Life Science*, vol. 28, no. 2, pp. 182–191, 2016.

[16] Q. Li, B. Shan, H. Li, J. Su, C. Zhang, and Q. Li, "Th17/Treg cell imbalance in patients with gastric cancer," *Chinese Journal of General Practice*, vol. 18, no. 29, pp. 3596–3600, 2015.

[17] F. Y. Zhang, N. Zhang, and L. Fang, "Effect of Qingrejiudhuatan decoction on quality of life in patients with advanced gastric cancer after operation," *World Journal of Integrated Chinese and Western Medicine*, vol. 13, no. 9, pp. 1286–1289 + 1317, 2018.

[18] D. Ju and P. Wei, "Medicinal mechanism and application of Clearing heat and detoxifying Traditional Chinese medicine in prevention and treatment of malignant tumor," *Jilin Traditional Chinese Medicine*, vol. 27, no. 1, pp. 60–62, 2007, in Chinese.

[19] L. Pan and P. Chen, "Research progress on antitumor mechanism of Qingrejiedu traditional Chinese medicine," *China Journal of Traditional Chinese Medicine*, vol. 25, no. 3, pp. 569–571, 2007, in Chinese.

[20] H. Lu and Z. Fang, "Research progress of heat clearing and detoxification therapy and its application in liver cancer," *Jiangsu Traditional Chinese Medicine*, vol. 22, no. 4, pp. 43–45, 2001, in Chinese.

[21] S. I. Grivennikov, F. R. Greten, and M. Karin, "Immunity, inflammation, and cancer," *Cell*, vol. 140, no. 6, pp. 883–899, 2010.

[22] D. Hanahan and R. A. Weinberg, "Hallmarks of cancer: the next generation," *Cell*, vol. 144, no. 5, pp. 646–674, 2011.

[23] H. F. Dvorak, "Tumors: wounds that do not heal-redux," *Cancer Immunology Research*, vol. 3, no. 1, pp. 1–11, 2015.

[24] R. Yasmin, S. Siraj, A. Hassan, A. R. Khan, R. Abbasi, and N. Ahmad, "Epigenetic regulation of inflammatory cytokines and associated genes in human malignancies," *Mediators of Inflammation*, vol. 2015, Article ID 201703, 8 pages, 2015.

[25] R. Maddaly, A. Subramaniyan, and H. Balasubramanian, "Cancer cytokines and the relevance of 3D cultures for studying those implicated in human cancers," *Journal of Cellular Biochemistry*, vol. 118, no. 9, pp. 2544–2558, 2017.

[26] L. C. L. T. van Kempen, D. J. Ruiter, G. N. P. van Muijen, and L. M. Coussens, "The tumor microenvironment: a critical determinant of neoplastic evolution," *European Journal of Cell Biology*, vol. 82, no. 11, pp. 539–548, 2003.

[27] K.-S. N. Atretkhany, M. S. Drutskaya, S. A. Nedospasov, S. I. Grivennikov, and D. V. Kuprash, "Chemokines, cytokines and exosomes help tumors to shape inflammatory

microenvironment," *Pharmacology & Therapeutics*, vol. 168, pp. 98–112, 2016.

[28] A. Vinocha, R. Grover, and R. Deepak, "Clinical significance of interleukin-6 in diagnosis of lung, oral, esophageal, and gall bladder carcinomas," *Journal of Cancer Research and Therapeutics*, vol. 14, no. 10, pp. 758–760, 2018.

[29] A. Babic, N. Schnure, N. P. Neupane et al., "Plasma inflammatory cytokines and survival of pancreatic cancer patients," *Clinical and Translational Gastroenterology*, vol. 9, no. 4, Article ID 145, 2018.

[30] N. R. West, S. McCuaig, F. Franchini, and F. Powrie, "Emerging cytokine networks in colorectal cancer," *Nature Reviews Immunology*, vol. 15, no. 10, pp. 615–629, 2015.

[31] N. Arora, O. Alsaied, P. Dauer et al., "Downregulation of Sp1 by Minnelide leads to decrease in HSP70 and decrease in tumor burden of gastric cancer," *PLoS One*, vol. 12, no. 2, Article ID e0171827, 2017.

[32] F. Lei, L. Zhang, Y. Ting, J. Jin, and W. Tao, "Study on anticancer activity of Polygonum cuspidatum," *Chinese Medicinal Materials*, vol. 29, no. 7, pp. 689–691, 2006, in Chinese.

[33] F. Zhang, N. Zhang, and F. Liang, "Effects of rhizoma tengilii root preparation on MMP-2, MMP-9 and SDF-1 expression of GASTRIC cancer CELLS SGC-7901," *Chinese Journal of Medicine*, vol. 33, no. 2, pp. 175–180, 20 18, in Chinese.

[34] D. Hui, M. Zongling, S. Rui, W. Tao, G. Xutao, and G. Ping, "Effect of root extract of Camellia japonicus on proliferation inhibition of human gastric cancer SGC7901 cells," *Chinese Journal of Gerontology*, vol. 37, no. 4, pp. 786–788, 2017.

[35] J. Bai, X. Wang, and Z. Ye, "Effects of extracts from the roots of Helicobacter pylori on apoptosis and Bcl-2 in human gastric cancer CELLS," *Journal of Shanxi University of Traditional Chinese Medicine*, vol. 35, no. 1, pp. 59–61, 2012, in Chinese.

[36] J. Gu, H. Zhang, L. Chen, S. Xu, G. Yuan, and X. Xu, "Drug-target network and polypharmacology studies of a Traditional Chinese Medicine for type II diabetes mellitus," *Computational Biology and Chemistry*, vol. 35, no. 5, pp. 293–297, 2011.

[37] K. Oh, M. Adnan, and D. Cho, "Uncovering mechanisms of *Zanthoxylum piperitum* fruits for the alleviation of rheumatoid arthritis based on network pharmacology," *Biology*, vol. 10, no. 8, Article ID 703, 2021.

[38] J. Ru, P. Li, J. Wang et al., "TCMSP: a database of systems pharmacology for drug discovery from herbal medicines," *Journal of Cheminformatics*, vol. 6, no. 1, Article ID 13, 2014.

[39] UniProt Consortium, "UniProt: the universal protein knowledgebase in 2021," *Nucleic Acids Research*, vol. 49, no. D1, pp. D480–D489, 2021.

[40] P. Shannon, A. Markiel, O. Ozier et al., "Cytoscape: a software environment for integrated models of biomolecular interaction networks," *Genome Research*, vol. 13, no. 11, pp. 2498–2504, 2003.

[41] G. Stelzer, N. Rosen, I. Plaschkes et al., "The GeneCards suite: from gene data mining to disease genome sequence analyses," *Current Protocols in Bioinformatics*, vol. 54, no. 1, pp. 1.30.1–1.30.33, 2016.

[42] J. S. Amberger and A. Hamosh, "Searching online mendelian inheritance in man (OMIM): a knowledgebase of human genes and genetic phenotypes," *Current Protocols in Bioinformatics*, vol. 58, no. 1, pp. 1.2.1–1.2.12, 2017.

[43] Y. Wang, S. Zhang, F. Li et al., "Therapeutic target database 2020: enriched resource for facilitating research and early development of targeted therapeutics," *Nucleic Acids Research*, vol. 48, no. D1, pp. D1031–D1041, 2020.

[44] D. S. Wishart, Y. D. Feunang, A. C. Guo et al., "DrugBank 5.0: a major update to the DrugBank database for 2018," *Nucleic Acids Research*, vol. 46, no. D1, pp. D1074–D1082, 2018.

[45] D. Szklarczyk, J. H. Morris, H. Cook et al., "The STRING database in 2017: quality-controlled protein-protein association networks, made broadly accessible," *Nucleic Acids Research*, vol. 45, no. D1, pp. D362–D368, 2017.

[46] D. Szklarczyk, A. L. Gable, D. Lyon et al., "STRING v11: protein-protein association networks with increased coverage, supporting functional discovery in genome-wide experimental datasets," *Nucleic Acids Research*, vol. 47, no. D1, pp. D607–D613, 2019.

[47] G. D. Bader and C. W. Hogue, "An automated method for finding molecular complexes in large protein interaction networks," *BMC Bioinformatics*, vol. 4, no. 1, Article ID 2, 2003.

[48] The Gene Ontology Consortium, "The gene Ontology resource: 20 years and still GOing strong," *Nucleic Acids Research*, vol. 47, no. D1, pp. D330–D338, 2019.

[49] M. Kanehisa and S. Goto, "KEGG: kyoto encyclopedia of genes and genomes," *Nucleic Acids Research*, vol. 28, no. 1, pp. 27–30, 2000.

[50] Y. Zhou, B. Zhou, L. Pache et al., "Metascape provides a biologist-oriented resource for the analysis of systems-level datasets," *Nature Communications*, vol. 10, no. 1, Article ID 1523, 2019.

[51] R. E. Buntrock, "ChemOffice ultra 7.0," *Journal of Chemical Information and Computer Sciences*, vol. 42, no. 6, pp. 1505-1506, 2002.

[52] H. M. Berman, J. Westbrook, Z. Feng et al., "The protein Data Bank," *Nucleic Acids Research*, vol. 28, no. 1, pp. 235–242, 2000.

[53] D. Seeliger and B. L. de Groot, "Ligand docking and binding site analysis with PyMOL and Autodock/Vina," *Journal of Computer-Aided Molecular Design*, vol. 24, no. 5, pp. 417–422, 2010.

[54] O. Trott and A. J. Olson, "AutoDock Vina: improving the speed and accuracy of docking with a new scoring function, efficient optimization, and multithreading," *Journal of Computational Chemistry*, vol. 31, no. 2, p. NA, 2009.

[55] T. Li, J. Fan, B. Wang et al., "TIMER: a web server for comprehensive analysis of tumor-infiltrating immune cells," *Cancer Research*, vol. 77, no. 21, pp. e108–e110, 2017.

[56] C. H. Mermel, S. E. Schumacher, B. Hill, M. L. Meyerson, R. Beroukhim, and G. Getz, "GISTIC2.0 facilitates sensitive and confident localization of the targets of focal somatic copy-number alteration in human cancers," *Genome Biology*, vol. 12, Article ID R41, 2011.

[57] R. Beroukhim, C. H. Mermel, D. Porter et al., "The landscape of somatic copy-number alteration across human cancers," *Nature*, vol. 463, pp. 899–905, 2010.

[58] Z. Wang, M. A. Jensen, and J. C. Zenklusen, "A practical guide to the cancer genome Atlas (TCGA)," *Methods in Molecular Biology*, vol. 1418, pp. 111–141, 2016.

[59] J. Wang and H. Cheng, "Application of clearing heat and detoxifying method and treating poison with poison in tumor treatment," *Chinese Journal of Traditional Chinese Medicine*, vol. 33, no. 8, pp. 3417–3419, 2018, in Chinese.

[60] D. Guo, N. Chen, P. Zhuo, B. Pan, and L.-B. Hou, "Suppressive effect of matrine on cell growth and decreases beta-catenin-dependent transcriptional activity in hepatoma cell

line Hep3B," *Journal of Chinese Medicinal Materials*, vol. 33, no. 5, pp. 778–781, 2010.

[61] Y.-H. Zheng, L.-H. Yin, T. H. M. Grahn, A.-F. Ye, Y.-R. Zhao, and Q.-Y. Zhang, "Anticancer effects of baicalein on hepatocellular carcinoma cells," *Phytotherapy Research*, vol. 28, no. 9, pp. 1342–1348, 2014.

[62] L.-H. Wei, J.-M. Lin, J.-F. Chu, H.-W. Chen, Q.-Y. Li, and J. Peng, "Scutellaria barbata D. Don inhibits colorectal cancer growth via suppression of Wnt/$\beta$-catenin signaling pathway," *Chinese Journal of Integrative Medicine*, vol. 23, no. 11, pp. 858–863, 2017.

[63] Y. Jin, W. Chen, H. Yang et al., "Scutellaria barbata D. Don inhibits migration and invasion of colorectal cancer cells via suppression of PI3K/Akt and TGF-2/Smad signaling pathways," *Experimental and Therapeutic Medicine*, vol. 14, no. 6, pp. 5527–5534, 2017.

[64] H.-Q. Wang, J.-J. Jin, and J. Wang, "Matrine induces mitochondrial apoptosis in cisplatin-resistant non-small cell lung cancer cells via suppression of $\beta$-catenin/survivin signaling," *Oncology Reports*, vol. 33, no. 5, pp. 2561–2566, 2015.

[65] C.-C. Chen, C.-P. Kao, M.-M. Chiu, and S.-H. Wang, "The anti-cancer effects and mechanisms of Scutellaria barbata D. Don on CL1-5 lung cancer cells," *Oncotarget*, vol. 8, no. 65, pp. 109340–109357, 2017.

[66] D. Hu, T. Ding, L. Jiang, L. Deng, S. Wu, and S. Mu, "Study on main constituents and antitumor activity of tripterygium wilfordii extract [J/OL]," *Guangxi Plant*, vol. 41, pp. 1–12, 2021, in Chinese.

[67] Y. Ma, T. Feng, Y. Han et al., "Research progress of antitumor mechanism and application of radix tengilii," *Journal of Traditional Chinese Medicine*, vol. 47, no. 6, pp. 118–121, 2019, in Chinese.

[68] J. He, L. Dong, B. Ma, W. Fengling, and T. Zhao, "Advances in the study of chemical constituents and antitumor pharmacological effects of the roots of Camellia japonicus," *Chinese Journal of Experimental Formulae*, vol. 21, no. 4, pp. 213–218, 2015, in Chinese.

[69] J. Zheng, Y. Xia, K. Shen, and B. Hu, "The antitumor effect and mechanism of the root of Podophyllum japonicum," *Chinese Journal of Traditional Chinese Medicine*, vol. 35, no. 10, pp. 2562–2564, 2017, in Chinese.

[70] Y. Wang, M. Li, Y. Xu, N. He, L. Leng, and Z. Li, "Tumor necrosis factor-$\alpha$ regulates matrix metalloproteinase-2 expression and cell migration via ERK pathway in rat glomerular mesangial cells," *Cell Biology International*, vol. 38, no. 9, 2014.

[71] T.-L. Hwang, L.-Y. Lee, C.-C. Wang, Y. Liang, S.-F. Huang, and C.-M. Wu, "Claudin-4 expression is associated with tumor invasion, MMP-2 and MMP-9 expression in gastric cancer," *Experimental and Therapeutic Medicine*, vol. 1, no. 5, pp. 789–797, 2010.

[72] T. Wang, J. Hou, S. Jian et al., "miR-29b negatively regulates MMP2 to impact gastric cancer development by suppress gastric cancer cell migration and tumor growth," *Journal of Cancer*, vol. 9, no. 20, pp. 3776–3786, 2018.

[73] E. I. Deryugina and J. P. Quigley, "Pleiotropic roles of matrix metalloproteinases in tumor angiogenesis: contrasting, overlapping and compensatory functions," *Biochimica et Biophysica Acta (BBA)-Molecular Cell Research*, vol. 1803, no. 1, pp. 103–120, 2010.

[74] N. Bagheri, M. Sadeghiani, G. Rahimian et al., "Correlation between expression of MMP-9 and MMP-3 in Helicobacter pylori infected patients with different gastroduodenal

diseases," *Arab Journal of Gastroenterology*, vol. 19, no. 4, pp. 148–154, 2018.

[75] X. Y. Pan and X. Li, "Study on the expression of matrix metalloproteinase-9 induced by Helicobacter pylori," *Chinese Journal of Medical Sciences*, vol. 6, no. 8, pp. 1061–1063, 2004.

[76] X. Wenmin, Z. Haiyan, H. Miao, and T. Jingyu, "Expression and significance of Cyclin D1 and MMP-9 in helicobacter pylori infected gastric cancer," *Journal of Clinical and Experimental Pathology*, vol. 35, no. 2, pp. 213–215, 2019.

[77] R. Deng, F. Mo, B. Chang et al., "Glucose-derived AGEs enhance human gastric cancer metastasis through RAGE/ERK/Sp1/MMP2 cascade," *Oncotarget*, vol. 8, no. 61, pp. 104216–104226, 2017.

[78] Y.-G. Shen, W. Feng, Y.-J. Xu et al., "Effects of RNA silencing of matrix metalloproteinase-2 on the growth of esophageal carcinoma cells *in vivo*," *Oncology Letters*, vol. 13, no. 3, pp. 1119–1124, 2017.

[79] E. Hadler-Olsen, A. I. Solli, A. Hafstad, J.-O. Winberg, and L. Uhlin-Hansen, "Intracellular MMP-2 activity in skeletal muscle is associated with type II fibers," *Journal of Cellular Physiology*, vol. 230, no. 1, pp. 160–169, 2015.

[80] T. Abbas and A. Dutta, "p21 in cancer: intricate networks and multiple activities," *Nature Reviews Cancer*, vol. 9, no. 6, pp. 400–414, 2009.

[81] S. Manickavinayaham, R. Velez-Cruz, A. K. Biswas, J. Chen, R. Guo, and D. G. Johnson, "The E2F1 transcription factor and RB tumor suppressor moonlight as DNA repair factors," *Cell Cycle*, vol. 19, no. 18, pp. 2260–2269, 2020.

[82] D. R. Robinson, Y.-M. Wu, and S.-F. Lin, "The protein tyrosine kinase family of the human genome," *Oncogene*, vol. 19, no. 49, pp. 5548–5557, 2000.

[83] K. L. Suen, X. R. Bustelo, T. Pawson, and M. Barbacid, "Molecular cloning of the mouse grb2 gene: differential interaction of the Grb2 adaptor protein with epidermal growth factor and nerve growth factor receptors," *Molecular and Cellular Biology*, vol. 13, no. 9, pp. 5500–5512, 1993.

[84] H. Bongartz, K. Gille, W. Hessenkemper et al., "The multi-site docking protein Grb2-associated binder 1 (Gab1) enhances interleukin-6-induced MAPK-pathway activation in an SHP2-, Grb2-, and time-dependent manner," *Cell Communication and Signaling*, vol. 17, no. 1, Article ID 135, 2019.

[85] Y. H. Kang, A. Biswas, M. Field, and S. B. Snapper, "STAT1 signaling shields T cells from NK cell-mediated cytotoxicity," *Nature Communications*, vol. 10, no. 1, Article ID 912, 2019.

[86] J. Xuefeng, C. Wenming, S. Daoping et al., "Effect of quercetin on epithelial-mesenchymal transformation in gastric cancer," *Chinese Journal of Gastroenterology*, vol. 21, no. 8, pp. 1030–1032, 2015, in Chinese.

[87] Z. Yu, L. He, Y. Chen, M.-Y. Wu, X.-H. Zhao, and Z.-Y. Wang, "Effects of quercetin on the expression of VEGF-C and VEGFR-3 in gastric cancer cell line MGC-803," *Journal of Cell and Molecular Immunology*, vol. 25, no. 8, pp. 678–680, 2009.

[88] M. C. Kim, H. J. Lee, B. Lim et al., "Quercetin induces apoptosis by inhibiting MAPKs and TRPM7 channels in AGS cells," *International Journal of Molecular Medicine*, vol. 33, no. 6, pp. 1657–1663, 2014.

[89] Ú. C. Mc Menamin, A. T. Kunzmann, M. B. Cook et al., "Hormonal and reproductive factors and risk of upper gastrointestinal cancers in men: a prospective cohort study within the UK Biobank," *International Journal of Cancer*, vol. 143, no. 4, pp. 831–841, 2018.

[90] M. R. Gubbels Bupp and T. N. Jorgensen, "Androgen-induced immunosuppression," *Frontiers in Immunology*, vol. 9, Article ID 794, 2018.

[91] K. Mierzejewska, S. Borkowska, E. Suszynska et al., "Hematopoietic stem/progenitor cells express several functional sex hormone receptors-novel evidence for a potential developmental link between hematopoiesis and primordial germ cells," *Stem Cells and Development*, vol. 24, no. 8, pp. 927–937, 2015.

[92] A. R. Green, F. F. T. Barros, T. M. A. Abdel-Fatah et al., "HER2/HER3 heterodimers and p21 expression are capable of predicting adjuvant trastuzumab response in HER2+ breast cancer," *Breast Cancer Research and Treatment*, vol. 145, no. 1, pp. 33–44, 2014.

[93] T. T. Junttila, R. W. Akita, K. Parsons et al., "Ligand-independent HER2/HER3/PI3K complex is disrupted by trastuzumab and is effectively inhibited by the PI3K inhibitor GDC-0941," *Cancer Cell*, vol. 15, no. 5, pp. 429–440, 2009.

[94] L. Arnould, M. Gelly, F. Penault-Llorca et al., "Trastuzumab-based treatment of HER2-positive breast cancer: an antibody-dependent cellular cytotoxicity mechanism?" *British Journal of Cancer*, vol. 94, no. 2, pp. 259–267, 2006.

[95] Y. Izumi, L. Xu, E. Di Tomaso, D. Fukumura, and R. K. Jain, "Herceptin acts as an anti-angiogenic cocktail," *Nature*, vol. 416, no. 6878, pp. 279-280, 2002.

[96] D.-Y. Oh and Y.-J. Bang, "Pertuzumab in gastrointestinal cancer," *Expert Opinion on Biological Therapy*, vol. 16, no. 2, pp. 243–253, 2016.

[97] R. Noy and J. W. Pollard, "Tumor-associated macrophages: from mechanisms to therapy," *Immunity*, vol. 41, no. 1, pp. 49–61, 2014.

[98] A. Mantovani, F. Marchesi, A. Malesci, L. Laghi, and P. Allavena, "Tumour-associated macrophages as treatment targets in oncology," *Nature Reviews Clinical Oncology*, vol. 14, no. 7, pp. 399–416, 2017.

[99] L. Yang and Y. Zhang, "Tumor-associated macrophages: from basic research to clinical application," *Journal of Hematology & Oncology*, vol. 10, no. 1, Article ID 58, 2017.

[100] S. Yin, J. Huang, Z. Li et al., "The prognostic and clinicopathological significance of tumor-associated macrophages in patients with gastric cancer: a meta-analysis," *PLoS One*, vol. 12, no. 1, Article ID e0170042, 2017.

[101] T. Yamaguchi, S. Fushida, Y. Yamamoto et al., "Tumor-associated macrophages of the M2 phenotype contribute to progression in gastric cancer with peritoneal dissemination," *Gastric Cancer*, vol. 19, no. 4, pp. 1052–1065, 2016.

[102] H. Zhang, X. Wang, Z. Shen, J. Xu, J. Qin, and Y. Sun, "Infiltration of diametrically polarized macrophages predicts overall survival of patients with gastric cancer after surgical resection," *Gastric Cancer*, vol. 18, no. 4, pp. 740–750, 2015.